CHAPTER 3

RESULTS AND DISCUSSION

3.1 Optimization of FI-HG-AAS parameters

The following chemical and physical parameters were optimized to achieve the best analytical performance of the HG-AAS system for the reliable quantification of As in plant samples.

To obtain a stable and robust analytical signal, the quartz cell atomizer and the EDL-lamp were allowed to warm up for at least 45 min before starting a measurement sequence. Additionally, the response of the HG-AAS system to a 10 μgl^{-1} As^{III} standard solution was determined each day before starting measurements. The typical peak of 10 $\mu gl^{-1}As^{III}$ standard solution is shown in Appendix D-1. Although the relative standard deviations (%RSD) of 10 μgl^{-1} As^{III} standard solution were relatively low for both measurements modes (< 2%), evaluating peak heights resulted in about 4 times lower sensitivity compared to results obtained using peak area (Table 3-1 and Figure 3-1). Therefore, the peak area was used throughout all experiments for quantifying instrumental response.

All instrumental parameters were optimized using 10 $\mu gl^{-1}As^{III}$ and As^{V} standard solutions, respectively.

Table 3-1 The signals obtained from peak height and peak area measurements

Concentration (μgl^{-1})	Peak height (%RSD)[a]	Peak area (%RSD)[a]
0	0.000 (0.0)	0.000 (0.0)
2	0.192 (1.8)	0.740 (1.1)
4	0.358 (0.3)	1.420 (0.3)
6	0.523 (0.5)	2.035 (0.4)
8	0.668 (1.0)	2.609 (1.0)

[a] Values given are the means (n=3).

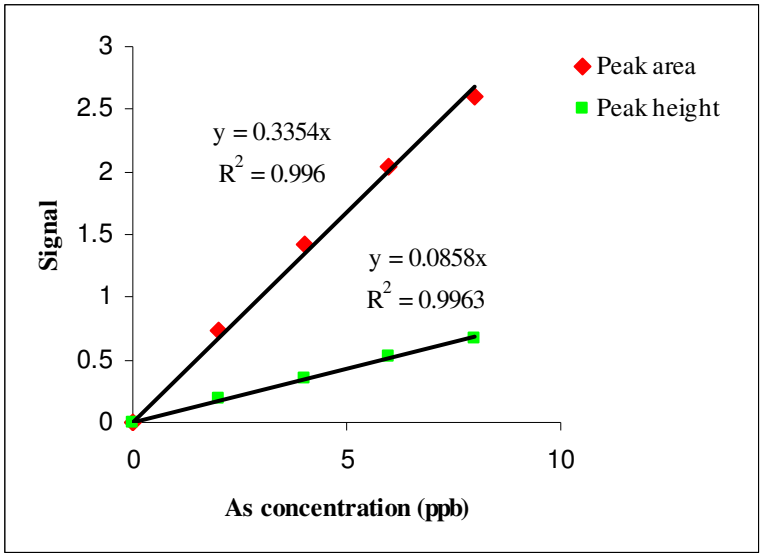

Figure 3-1 The signals obtained from peak height and peak area measurements

3.1.1 Effect of carrier gas flow rate

Argon is needed as carrier gas to transport the formed hydride to the quartz cell atomizer. The carrier gas flow rate influences generally to the sensitivity of the analysis, since increasing the flow rate of carrier gas can affect resting time of arsenic atoms in the atomizer cell. The gas flow rate settings in the employed HG-AAS instrument can only be increased in 40 $mlmin^{-1}$ increments up to a maximum gas flow rate of 200 $mlmin^{-1}$. As shown in Table 3-2 and Figure 3-2, when the gas flow rate was increased from 40-100 $mlmin^{-1}$ the signal intensities for the As standard solution significantly decreased with the maximum at 40 $mlmin^{-1}$. Therefore, a gas flow rate of 40 $mlmin^{-1}$ was used for all further investigations.

Table 3-2 Influence of carrier gas flow rate on signal of 10 μg l^{-1} As^{III} standard solution

Flow rate ($mlmin^{-1}$)	Peak area[a]	%RSD
0	1.839	1.3
40	2.817	0.4
50	2.644	0.2
75	2.404	0.9
100	2.104	0.0

[a] Values given are the means (n=3).

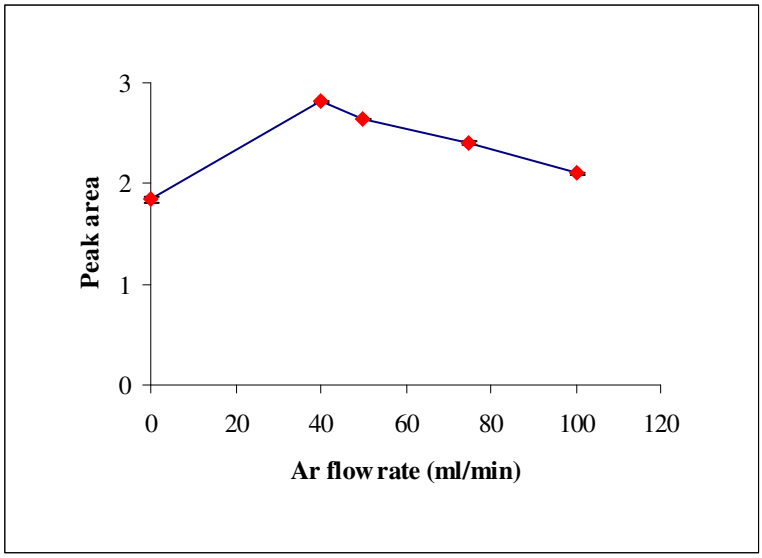

Figure 3-2 Influence of carrier gas flow rates on signal of 10 μg l^{-1} As^{III} standard solution

3.1.2 Effect of HCl concentrations

The HCl concentration is an important parameter because it significantly influences the HG efficiency. The concentration of HCl, acting as a carrier solution, was investigated within the range 1-20 % (v/v) to obtain highest signal intensities for As standard solution. As shown in Table 3-3 and Figure 3-3, the signals for As^{III} standard solutions reached a maximum at a HCl concentration of 10 % (v/v) and then decreased. However, the HCl

concentration of 5% (v/v) was chosen for all further investigations since the signal for As standard solution obtained was not significantly different from that obtained from the HCl concentration of 10 % (v/v).

Table 3-3 Influence of HCl concentrations on hydride generation reaction

HCl concentration (%v/v)	Peak area[a]	%RSD
1	2.825	1.0
5	2.907	0.2
10	2.933	0.7
20	2.919	0.5

[a] Values given are the means (n=3).

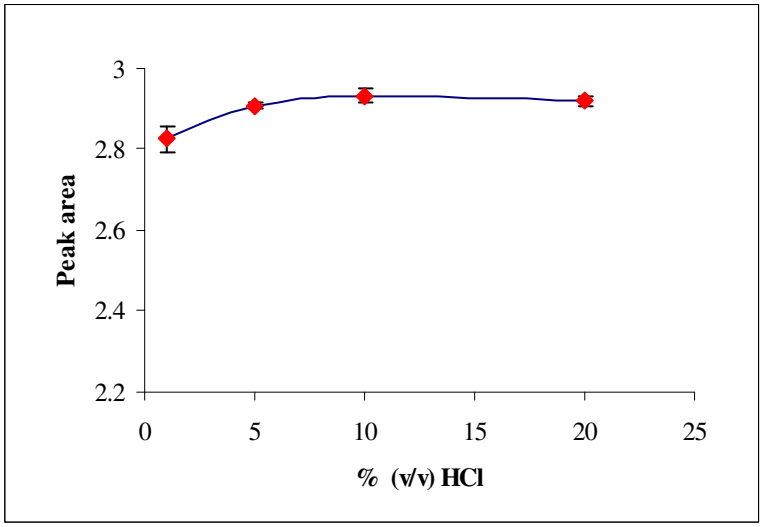

Figure 3-3 Influence of HCl concentrations on hydride generation reaction

3.1.3 Effect of $NaBH_4$ concentrations

The $NaBH_4$ concentrations are also considered to be important parameters that significantly influence the HG efficiency. Optimization of $NaBH_4$ concentration was carried out between 0.1-0.7 % (w/v) using the optimized HCl concentration of 5% (v/v). As shown in Table 3-4 and Figure 3-4, the signal intensities increased up to a concentration of 0.3% (w/v) $NaBH_4$ and then significantly decreased. Therefore, $NaBH_4$ of 0.3% (w/v) was used as optimal concentration for further investigations.

Table 3-4 Influence of $NaBH_4$ concentrations on hydride generation reaction

$NaBH_4$ concentration (%w/v)	Peak area[a]	%RSD
0.1	2.992	0.7
0.3	3.301	0.3
0.5	2.911	0.1
0.7	2.698	0.8

[a] Values given are the means (n=3).

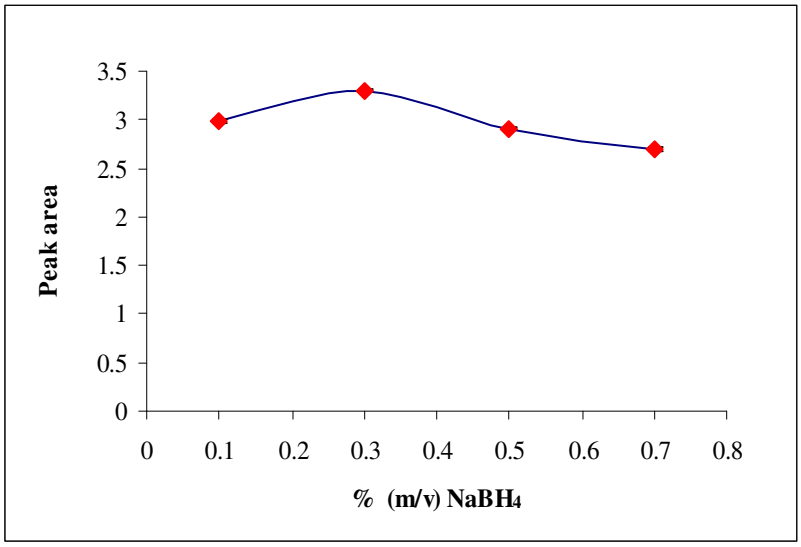

Figure 3-4 Influence of $NaBH_4$ concentrations on hydride generation reaction

3.1.4 Effect of As^{V} over As^{III} detection

For the selective determination of As^{III}, the evaluation of the As^{V} interference effect was performed. With mixtures containing 10 μgl^{-1} of As^{III} with corresponding relative contents of 1, 2, 3, 4, 5, 6, 7, 8, 9, 10 and 20 μgl^{-1} of As^{V}. Results from Table 3-5 and Figure 3-5 showed that the As^{V} dose not interfere As^{III} detection even at two times higher concentration of As^{V} to As^{III}. Therefore, the proposed methodology for As^{III} speciation can be applied to samples with high As^{V} levels.

Table 3-5 Influence of As^{V} over As^{III} determination

As^{V}:As^{III} concentration (μgl^{-1})	%Recovery of As^{III}[a]	%RSD
1:10	95.43	1.3
2:10	95.45	0.4
3:10	101.40	0.2
4:10	98.07	0.3
5:10	98.33	0.2
6:10	98.15	0.4
7:10	96.94	0.4
8:10	99.19	0.3
9:10	100.90	0.2
10:10	102.90	0.3
20:10	98.45	0.4

[a] Values given are the means (n=3).

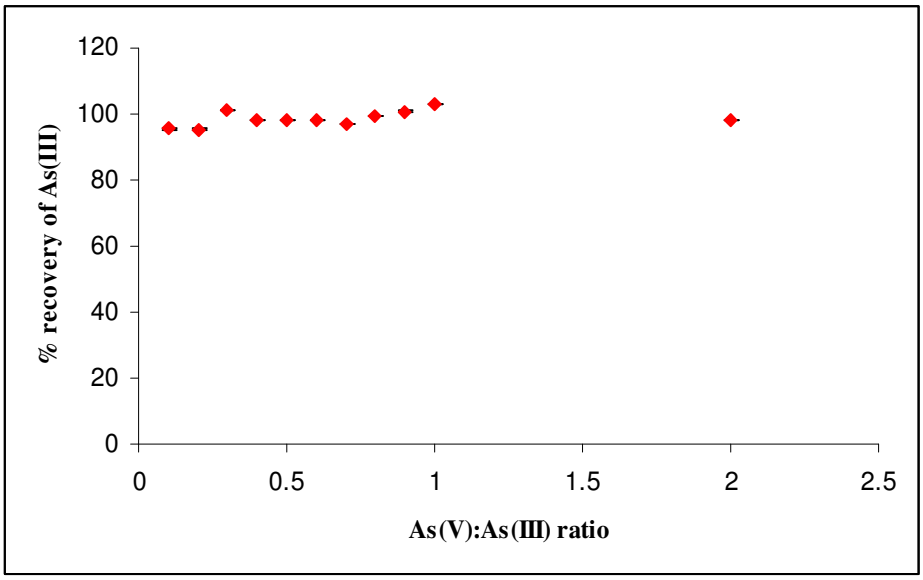

Figure 3-5 Influence of As^{V} over As^{III} determination

3.1.5 KI/ascorbic acid concentrations

In the pre-reduction process, various concentrations of KI (0-9%, w/v) stabilized with ascorbic acid (5%, w/v) were tested. It was found that As signal intensities increased with increasing amounts of KI/ascorbic acid added, and was stable when the amounts of KI/ascorbic acid were greater than 1% (w/v), as shown in Table 3-7 and Figure 3-7. However**,** the KI/ascorbic acid concentration of 3% (w/v) was chosen to make sure that KI/ascorbic acid concentration is sufficient for the quantitative pre-reduction of As^{V} to As^{III}. The reduction of As^{V} with KI was shown in the reaction 2-1 of chapter 2.

Table 3-6 Influence of KI/ascorbic acid concentrations on hydride generation reaction

KI concentration (%w/v)	Peak area[a]	%RSD
0	0.307	1.7
1	2.627	0.2
3	2.610	0.1
5	2.580	0.9
7	2.539	1.0
9	2.261	2.9

[a] Values given are the means (n=3).

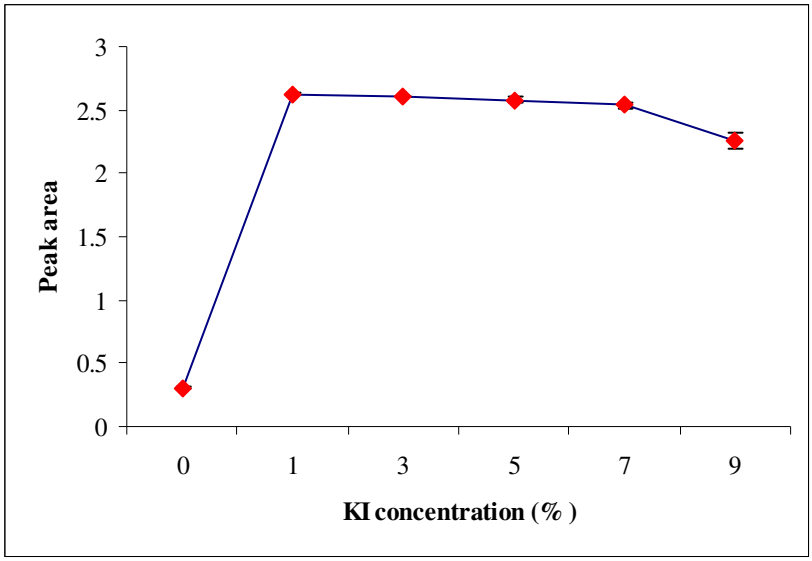

Figure 3-6 Influence of KI/ascorbic acid concentrations on hydride generation reaction

3.1.6 Effect of reducing time

To determine the time required to quantitatively reduce As^{V} to As^{III}, the reduction time was varied from 0 to 75 min with a sample containing 10 $\mu g l^{-1} As^{V}$ and 3% (w/v) KI/ascorbic acid. It was found that arsenic response was stable for reduction times greater than 30 s, as shown in Table 3-7 and Figure 3-7. Thus the reduction time of 45 s was chosen to allow relatively quantitative reduction of As^{V} to As^{III} in the sample solution.

Table 3-7 Influence of time on the reduction of As^{V} to As^{III}

Times (min)	Peak area[a]	%RSD
0	0.285	0.2
15	2.893	0.8
30	3.025	1.4
45	3.180	0.5
60	3.166	0.3
75	3.049	1.0

[a] Values given are the means (n=3).

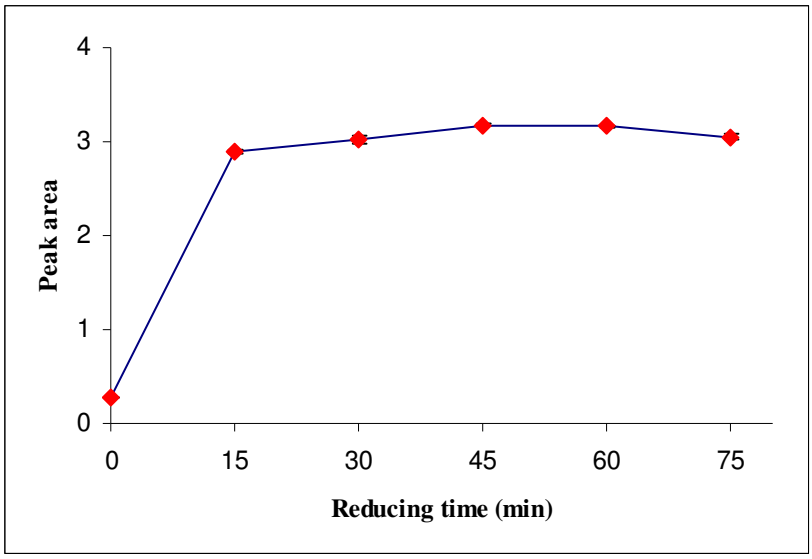

Figure 3-7 Influence of time on the reduction of As^{V} to As^{III}

3.1.7 Efficiency of reduction of As^{V} to As^{III}

The study of the efficiency of the reduction of As^{V} to As^{III} revealed that As^{V} can be converted to As^{III} almost 100% as shown in Table 3-8 and Figure 3-8 to such an extent that it is reasonable to state that the reduction of As^{V} to As^{III} is quantitative. However, the efficiency was

gradually decreased with increasing of As^{V} concentration. As^{V} concentration less than 20 μgl^{-1} was therefore recommended for total-As determinations. In the case of As^{V} concentration higher than 20 μgl^{-1}, increasing KI/ascorbic acid amount was necessary.

Table 3-8 The efficiency of the conversion of As^{V} to As^{III}

As^{V} concentration added (μgl^{-1})	%Recovery of As^{V} [a]	%RSD
2	106.90	0.4
4	101.73	0.1
6	98.03	1.8
8	96.83	0.2
10	96.12	0.6
15	88.29	0.8
20	79.70	1.6

[a] Values given are the means (n=3).

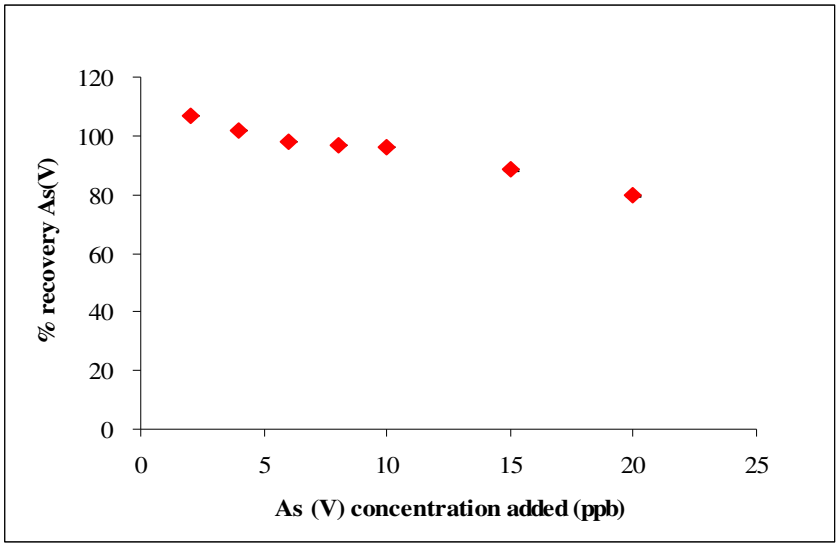

Figure 3-8 The efficiency of the conversion of As^{V} to As^{III}

3.2 Analytical performances data for FI-HG-AAS

3.2.1 Linear range

The linear range is determined by plotting the peak area versus the concentration of As standard solution. It is desirable to work within the linear region of the resulting calibration curve (AAnalyst 800, Perkin-Elmer).

3.2.1.1 Linear range of As^{III} detection

The calibration graph of As^{III} at various concentrations (0-40 μgl^{-1}) is shown in Table 3-9 and Figure 3-9 (a). It was found that the curve was linear from 0 to at least 20 μgl^{-1} with the correlation coefficient (r^2) of 0.9985 as shown in Figure 3-9 (b) and gradually became non linear with increasing of As^{III} concentrations.

3.2.1.2 Linear range of TAs detection

The calibration graph of TAs at various concentrations (0-40 μgl^{-1}) is shown in Table 3-10 and Figure 3-10 (a). It was found that the curve was linear from 0 to at least 20 μgl^{-1} with the correlation coefficient (r^2) of 0.9955 as shown in Figure 3-9 (b) and gradually became non linear with increasing of As concentrations.

Table 3-9 The peak area of As^{III} detection at different As^{III} concentrations

As^{III} concentration (μgl^{-1})	Peak area[a]	%RSD
0	0.000	0.0
1	0.197	1.6
2	0.480	0.4
4	1.137	0.1
6	1.529	0.3
8	2.215	0.1
10	2.818	0.4
12	3.287	0.5
14	3.839	0.2
16	4.266	0.4
18	4.817	1.0
20	5.304	0.1
22	6.264	0.3
24	6.598	0.9
26	7.062	0.4
28	7.209	0.3
30	7.470	0.3
32	7.537	0.2
34	8.003	0.9
36	8.248	0.6
38	8.404	0.3
40	8.659	0.8

[a] Values given are the means (n=3).

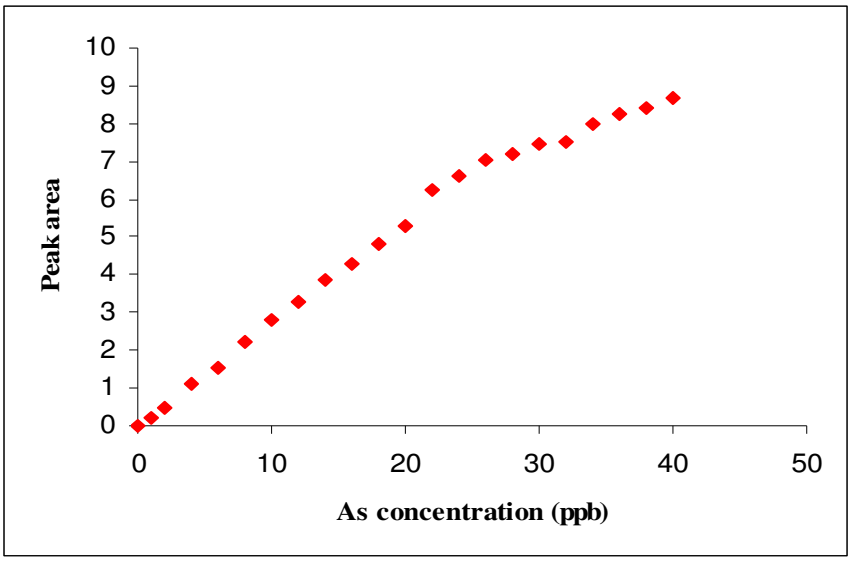

(a)

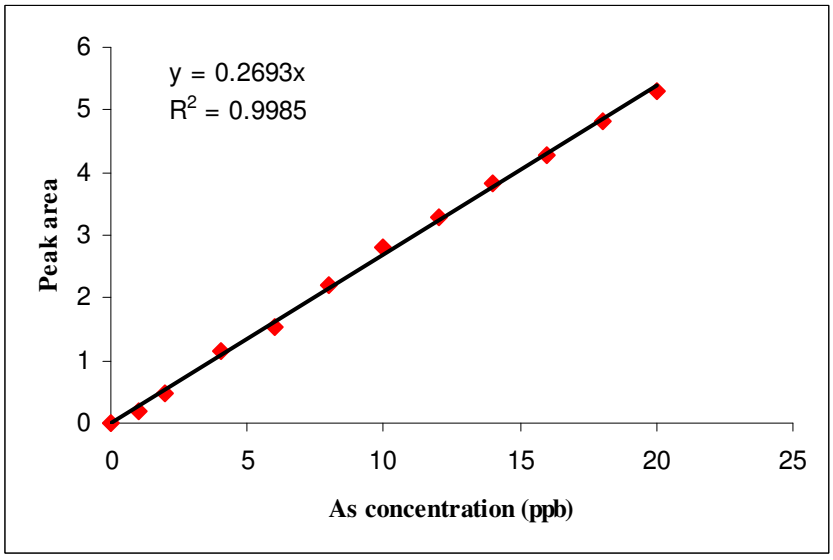

(b)

Figure 3-9 The calibration graph of As^{III} at the different concentrations; (a) 0-40 μgl^{-1}, (b) 0-20 μgl^{-1}

Table 3-10 The peak area of TAs detection at different As^{V} concentrations

As concentration (μgl^{-1})	Peak area[a]	%RSD[a]
0	0.000	0.0
1	0.399	0.9
2	0.628	1.3
4	1.214	0.4
6	1.653	0.3
8	2.144	1.5
10	2.471	1.9
12	2.894	4.3
14	3.521	3.6
16	3.835	0.5
18	4.228	0.1
20	4.610	0.1
22	4.812	1.2
24	4.940	1.2
26	5.059	0.2
28	5.191	0.1
30	5.367	0.4
32	5.443	0.3
34	5.466	0.9
36	5.513	0.3
38	5.734	1.4
40	5.574	0.1

[a] Values given are the means (n=3).

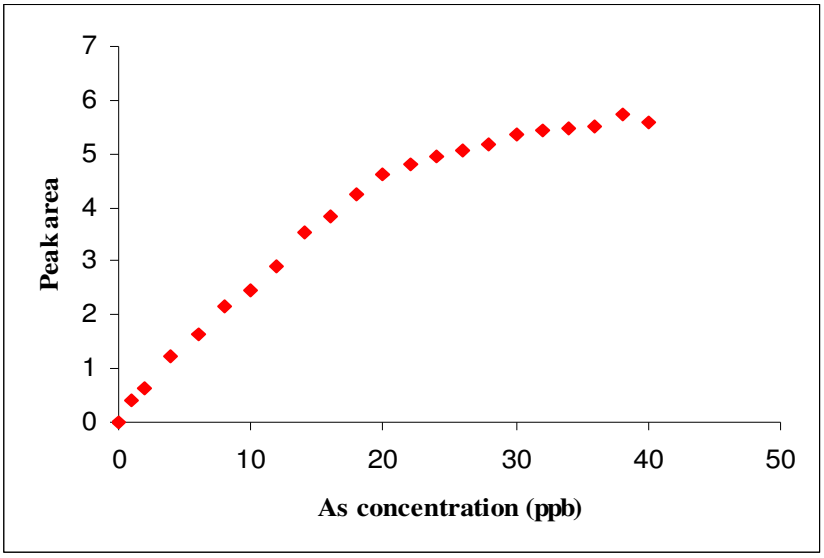

(a)

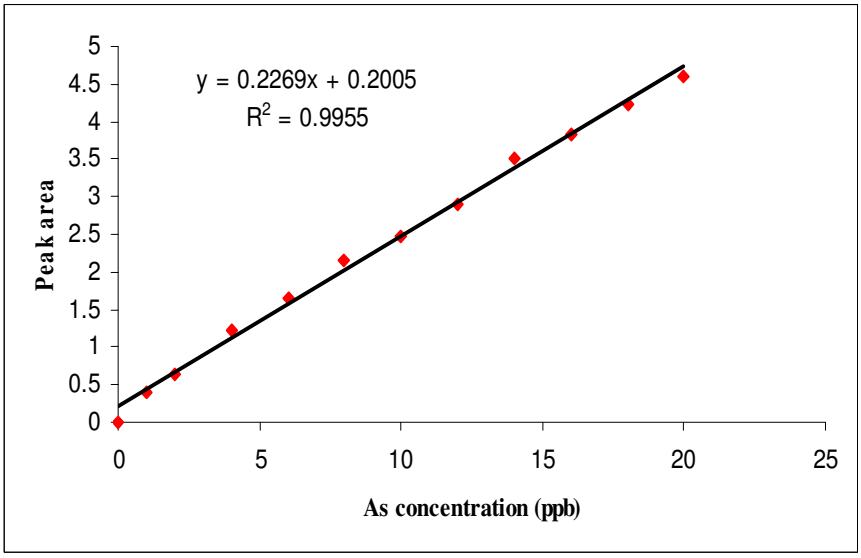

(b)

Figure 3-10 The calibration graph of TAs at the different concentrations; (a) 0-40 $\mu g l^{-1}$, (b) 0-20 $\mu g l^{-1}$

3.2.2 Limit of detection (LOD) and Limit of quantification (LOQ)

The limits of detection (LOD) and limits of quantitative (LOQ) of As^{III} and TAs were studied by measuring the absorbance of ten replications of blank. The limits of detection and limits of quantitative were calculated from the equation in section 2.6.2 and 2.6.3, respectively (Coelho *et al*., 2002).

The results for evaluating LOD and LOQ of As^{III} and TAs are shown in Table 3-11 and Table 3-12, respectively.

3.2.1.1 LOD and LOQ of As^{III} determination

From Table 3-11, when ten blanks were measured and the slope from calibration graph was obtained, it was found that the LOD and LOQ of As^{III} were 0.02 and 0.07 μgl^{-1}, respectively.

3.2.1.2 LOD and LOQ of TAs determination

From Table 3-12, when ten blanks were measured and the slope from calibration graph was obtained, it was found that the LOD and LOQ of TAs were 0.03 and 0.10 μgl^{-1}, respectively.

Table 3-11 The determination of 10 blanks for LOD and LOQ quantification (As^{III}) by FI-HG-AAS

Replicate	**Peak area**	
1	0.002	
2	0.005	
3	0.003	
4	0.001	
5	0.006	
6	0.005	
7	0.005	
8	0.004	
9	0.005	
10	0.008	
Average	**0.004**	
SD (σ)	**0.002**	
Calibration Slope (m)	**0.275**	
LOD (3σ/m)	**0.02**	**(μgl^{-1})**
LOQ (10σ/m)	**0.07**	**(μgl^{-1})**

Table 3-12 The determination of 10 blanks for LOD and LOQ quantification (TAs) by FI-HG-AAS

Replicate	**Peak area**	
1	0.054	
2	0.053	
3	0.055	
4	0.056	
5	0.059	
6	0.054	
7	0.051	
8	0.053	
9	0.054	
10	0.059	
Average	**0.055**	
SD (σ)	**0.003**	
Calibration Slope (m)	**0.277**	
LOD (3σ/m)	**0.03**	**($\mu g l^{-1}$)**
LOQ (10σ/m)	**0.10**	**($\mu g l^{-1}$)**

3.2.3 Accuracy and precision

The accuracy of this investigation method was evaluated from the determination of certified reference material (CTA-VTL-2; Virginia Tobacco Leaves) with a certified total arsenic concentration of 0.969 ± 0.072 $\mu g g^{-1}$. The descriptions of CTA-VTL-2 are shown at Appendix D-2). As shown in Table 3-13, total acid-digested arsenic determination in CTA-VTL-2 (Virginia Tobacco Leaves) was 0.961 ± 0.061 $\mu g g^{-1}$, which was in good agreement with the certified value (0.969 ± 0.072 $\mu g g^{-1}$). The recovery of As was 99%.

Table 3-13 The experimental and certified values for As determination in the CRM by FI-HG-AAS

Sample	**Certified value** ($\mu g g^{-1}$)	**Determined value** ($\mu g g^{-1}$)	**%recovery**
CTA-VTL-2	0.969±0.072	0.961±0.061	99

However, for inorganic arsenic speciation, no certified value of concentration has been provided for inorganic arsenic species (As^{III} and As^{V}). Therefore, the recovery values of inorganic species were quantified by spiking 1, 10 and 20 $\mu g l^{-1}$ of As^{III} and As^{V} to samples. As shown in Table 3-14, the recovery values for As^{III} and As^{V} were in agreement with the value of spiked samples.

Table 3-14 Experimental recovery on arsenic determination by FI-HG-AAS in edible plant samples spiked with 1, 10 and 20 $\mu g l^{-1}$ of As^{III} and As^{V}

	As^{III}		As^{V}	
	Conc. ($\mu g l^{-1}$)	Recovery (%)	Conc. ($\mu g l^{-1}$)	Recovery (%)
Sample	1.0	-	0.6	-
Sample+1 $\mu g l^{-1}$	1.9	90	1.7	110
Sample+10 $\mu g l^{-1}$	12.5	115	10.7	101
Sample+20 $\mu g l^{-1}$	22.9	110	19.2	93

In addition, the precision of the method was also evaluated as %RSD of nine replicates. Satisfactory results are shown in Table 3-15 and Table 3-16. The %RSD of 10 μgl^{-1} As^{III} and TAs determinations obtained by this method were 2 and 4%, respectively.

Table 3-15 The determination of 10 μgl^{-1} As^{III} for evaluating the precision

Replicate	**Peak area**
1	3.313
2	3.298
3	3.292
4	3.309
5	3.271
6	3.268
7	3.326
8	3.194
9	3.140
Average	**3.268**
SD	**0.062**
%RSD	**2**

Table 3-16 The determination of 10 μgl^{-1} TAs for evaluating the precision

Replicate	**Peak area**
1	2.569
2	2.559
3	2.566
4	2.707
5	2.563
6	2.528
7	2.595
8	2.417
9	2.402
Average	**2.545**
SD	**0.092**
%RSD	**4**

3.2.4 Recovery

The percent recovery of total inorganic arsenic (As^{III} and As^{V}) in the water-extracted edible plant samples was studied in section 2.6.6 and the results are shown in Table 3-17. The recovery values by spiking 1 μgl^{-1} and 10 μgl^{-1} of As^{III} and As^{V} were found to be greater than 94% of total inorganic arsenic.

Table 3-17 The determination of spiked samples

$As^{III}+As^{V}$ concentration spiked (μgl^{-1})	%Recovery of TAs [a]
Lemon grass	
1+1	102
10+10	104
Turmeric	
1+1	94
10+10	96

[a] Values given are the means (n=3).

3.3 Determination of As species in edible plant samples using FI-HG-AAS

For the determination of arsenic concentration in samples, first of all concentrations of the arsenic species in the extracted and digested samples were calculated using both external calibration and standard addition methods. As shown in Appendix D-3, it was found that significant differences were observed between the slopes of the external calibration and the standard addition calibration lines (*t*-test, $P<0.05$). Therefore, the standard addition method was used to determine the arsenic in samples to minimize the effect of the chemical composition of the matrix.

The FI-HG-AAS method was applied to determine of inorganic arsenic species in 30 samples of two types of edible plants (Lemongrass 15 samples and Turmeric 15 samples) collected from arsenic contaminated area, Ron Phibun sub-district, Ron Phibun district, Nakhon Si Thammarat province. The concentrations of arsenic found in Lemon grass and Turmeric are shown in Table 3-18 and Table 3-19, respectively. Arsenic contents were found to be 0.01 to 0.39 μgg^{-1} and 0.06 to 0.21 μgg^{-1} in Lemongrass, and from 0.02 to 0.33 μgg^{-1} and 0.06 to 0.20 μgg^{-1} in Turmeric for As^{III} and As^{V}, respectively. It can reasonably be stated that As^{III} and As^{V} contents found in both samples do not exceed the food safety limits for Thailand and several countries (Table 3-20). The concentrations of total acid-digested arsenic in Lemongrass and Turmeric from this study were in the same range as those reported by Khoomrung (2006).

Moreover, it was observed that there were large differences between the total water-extracted arsenic (As^{III} + As^{V}) and total acid-digested arsenic (inorganic arsenic + organic arsenic) in edible plant samples which may result from following reasons: (i) The extraction efficiency of arsenic from edible plants (total water-soluble arsenic) was not high enough, (ii) There could possibly be non water-soluble arsenolipids in terrestrial plants (Zhao *et al*., 2006) and (iii) It is also possible that some arsenic is bound to SH groups of cytosolic proteins and macromolecular constituents (Styblo *et al*., 1996).

In previous study of Zhao and co-worker, they have stated to the solubility of arsenic compounds that As^{III}, As^{V}, MMAA, DMAA and TAMO have been classified to be water-soluble compounds whereas arsenolipids have been classified to be non water-soluble compounds (lipid-soluble). The predominant forms of water-soluble arsenic in terrestrial plants are inorganic arsenic forms, As^{III} and As^{V} (Appendix D-4). This reflects that most terrestrial plants do not have a biochemical process to convert inorganic arsenic to less toxic organoarsenic compounds and hence no methylated arsenic (i.e. MMAA, DMAA, TMAO) is present (Zhao *et al*., 2006). From the details mentioned above, it may be concluded that all extractable water-soluble arsenic in test plants of this work are present in inorganic forms. In addition, it can be also concluded that non water-soluble arsenic found in both Lemongrass and Turmeric was higher than water-soluble arsenic.

Table 3-18 Concentrations of total-As and inorganic arsenic species in Lemon grass (as $\mu g g^{-1}$ dry weight, mean±SD)

Villages/point	As^{III}	As^{V}	Total water-extracted As[a]	Total acid-digested As[b]
M.1/1	0.026±0.002	0.114±0.010	0.140±0.009	0.238±0.023
M.1/2	0.020±0.002	0.102±0.009	0.122±0.012	0.226±0.002
M.1/3	0.031±0.004	0.092±0.012	0.123±0.014	0.316±0.010
M.1/4	0.038±0.003	0.213±0.016	0.251±0.019	0.304±0.005
M.1/5	0.036±0.004	0.093±0.013	0.129±0.010	0.247±0.000
M.2/1	0.034±0.003	0.091±0.009	0.125±0.009	0.381±0.008
M.2/2	0.038±0.002	0.058±0.009	0.096±0.011	0.231±0.007
M.2/3	0.049±0.004	0.065±0.011	0.114±0.010	0.301±0.006
M.2/4	0.385±0.014	0.061±0.033	0.446±0.019	0.979±0.009
M.2/5	0.040±0.004	0.068±0.013	0.108±0.009	0.465±0.008
M.13/1	0.022±0.002	0.094±0.005	0.116±0.003	0.339±0.007
M.13/2	0.023±0.002	0.120±0.015	0.143±0.017	0.281±0.007
M.13/3	0.010±0.000	0.106±0.009	0.116±0.009	0.148±0.005
M.13/4	0.036±0.003	0.066±0.009	0.102±0.007	0.175±0.008
M.13/5	0.022±0.002	0.114±0.017	0.136±0.016	0.197±0.004

[a] Total water-soluble inorganic arsenic species (As^{III} + As^{V}) extracted by water.

[b] Total arsenic (all species) was determined by digesting samples with a $HNO_3/HClO_4/H_2SO_4$ mixture at 100 ^{o}C.

Table 3-19 Concentrations of total-As and inorganic arsenic species in Turmeric (as $\mu g g^{-1}$ dry weight, mean±SD)

Villages/sites	As^{III}	As^{V}	Total water-extracted As[a]	Total acid-digested As[b]
M.1/1	0.041±0.005	0.064±0.009	0.105±0.005	0.601±0.017
M.1/2	0.026±0.002	0.065±0.003	0.091±0.005	0.365±0.012
M.1/3	0.025±0.000	0.086±0.009	0.091±0.009	0.290±0.017
M.1/4	0.023±0.002	0.105±0.014	0.128±0.012	0.623±0.005
M.1/5	0.053±0.003	0.157±0.024	0.210±0.026	0.660±0.022
M.2/1	0.020±0.002	0.144±0.003	0.110±0.005	0.468±0.011
M.2/2	0.162±0.003	0.144±0.014	0.306±0.013	0.997±0.006
M.2/3	0.026±0.002	0.059±0.008	0.085±0.010	0.563±0.019
M.2/4	0.075±0.008	0.076±0.015	0.151±0.008	0.557±0.003
M.2/5	0.021±0.002	0.130±0.019	0.151±0.018	1.384±0.008
M.13/1	0.024±0.002	0.066±0.003	0.090±0.005	0.497±0.014
M.13/2	0.026±0.002	0.090±0.010	0.116±0.012	1.077±0.010
M.13/3	0.088±0.011	0.199±0.031	0.287±0.026	0.597±0.006
M.13/4	0.038±0.003	0.088±0.004	0.126±0.007	0.396±0.004
M.13/5	0.334±0.022	0.146±0.053	0.480±0.048	1.873±0.005

[a] Total water-soluble inorganic arsenic species (As^{III} + As^{V}) extracted by water.

[b] Total arsenic (all species) was determined by digesting samples with a $HNO_3/HClO_4/H_2SO_4$ mixture at 100 ^{o}C.

Table 3-20 The maximum contamination level of arsenic in food for several countries

Countries	**Maximum contamination level ($\mu g g^{-1}$)**
China	0.5
Japan	1-3.5
Kenya	1-2
Singapore	1
Thailand	2

Source: http://elib.fda.moph.go.th/library/fulltext/public/2729/doo2.gif (20/12/2005)

3.4 Optimization of CSV parameters

Before the optimization of parameters of CSV was carried out, a comparison between differential pulse and square wave mode (DPCSV and SWCSV) was firstly performed. A comparison of CSV modes of As^{III} determinations in the presence of Cu^{II} (as shown in Figure 3-11) indicated that square wave mode resulted in about 5 times higher sensitivity than differential pulse mode. Subsequently, SWCSV was chosen to use for all experiments.

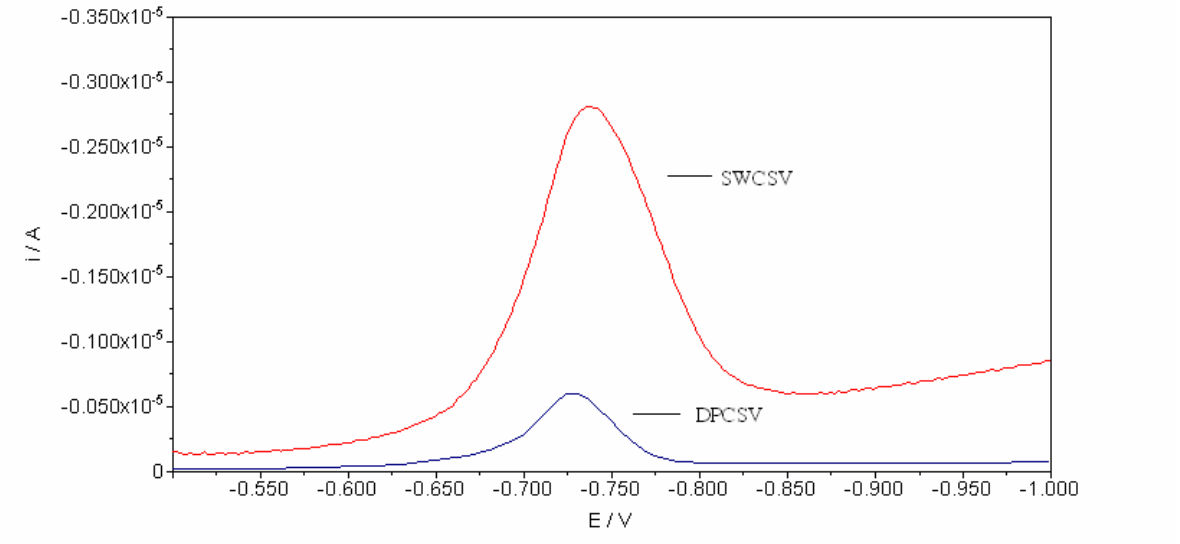

(a)

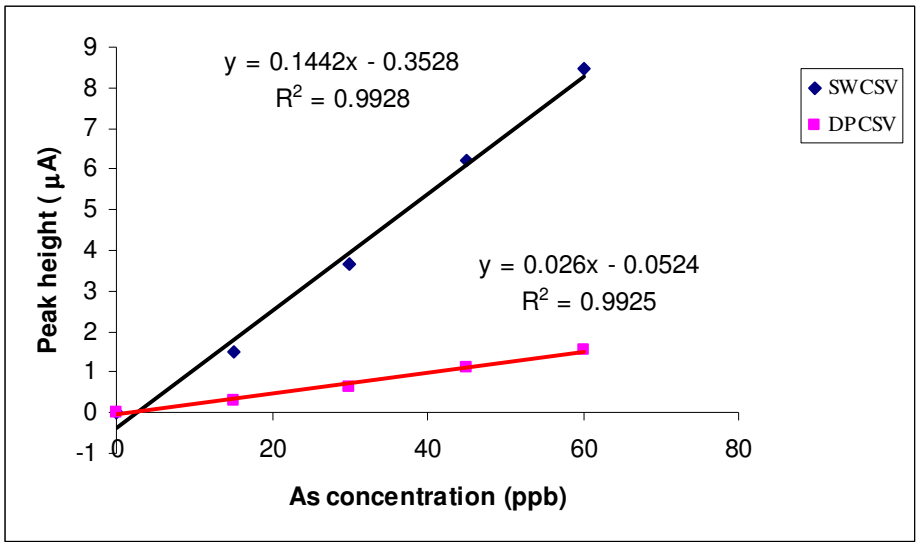

(b)

Figure 3-11 A comparison between SWCSV and DPCSV mode; (a) the linear sweep voltammograms and (b) the calibration graphs of each mode

In addition, the peak area has the sensitivity about 10 times lower than the peak height (Figure 3-12). Therefore, the peak height was used throughout all experiments for quantifying instrumental response.

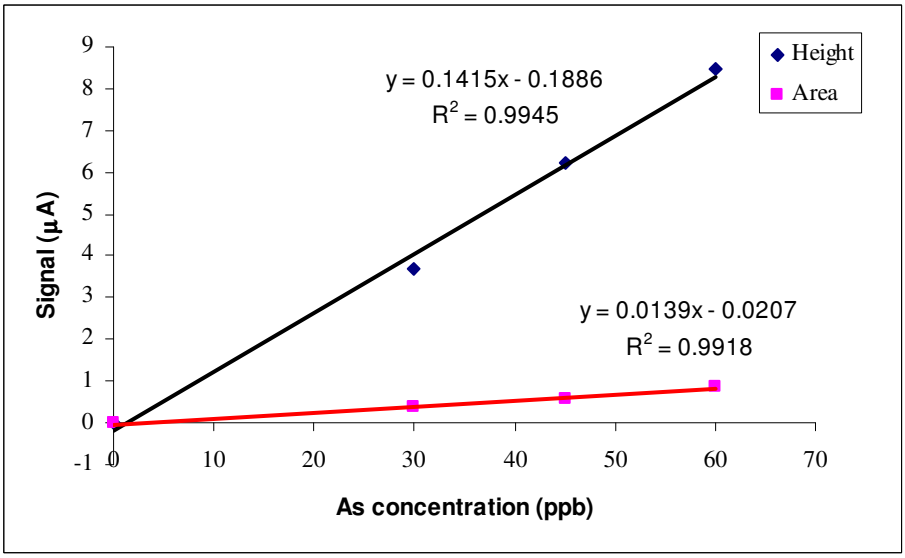

Figure 3-12 A comparison between peak height and peak area for SWCSV mode

The following chemical and physical parameters were optimized to achieve the best analytical performance of the CSV system for the reliable quantification of As in plant samples.

3.4.1 Deposition potential

In As^{III} determination, SWCSV deposition potential was investigated by varying the potential from -0.30 to -0.50 V versus reference electrode. For As concentration 20 μgl^{-1} and 50 mgl^{-1} Cu^{II}, the results were shown in Table 3-21 and Figure 3-13. It was found that peak response initially increased and then decreased, maximizing at -0.38 V. The same potential was found to give maximum response by Ferreira and Barros (Ferreira and Barros, 2002) and it is therefore selected in this work.

Table 3-21 Influence of deposition potential on As^{III} peak height ($E_{1/2} \approx$ -0.680 to -0.724 V)

Deposition potential (V)	Peak height (μA)	%RSD
-0.30	0.162	1.2
-0.32	0.248	0.2
-0.34	1.071	2.8
-0.36	1.412	3.8
-0.38	2.788	0.9
-0.40	1.734	0.0
-0.42	0.281	6.2
-0.44	0.008	0.0
-0.46	0.003	0.0
-0.48	0.326	3.8
-0.50	0.309	4.9

[a] Values given are means (n=3).

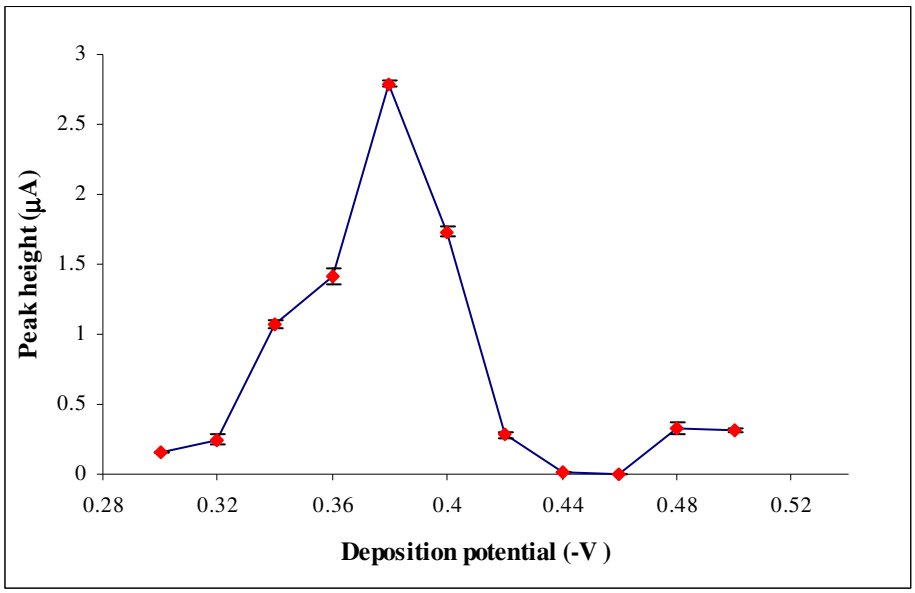

Figure 3-13 Influence of deposition potential on As^{III} peak height ($E_{1/2} \approx$ -0.680 to -0.724 V)

In case of TAs determination, initially the same deposition potential (-0.38 V) previously obtained for the determination of As^{III} was adopted. It was found that in the presence of thiosulfate (reducing agent) and high concentration of Cu^{II} (400 mgl^{-1}), the peak current decreased. Therefore, SWCSV deposition potential was investigated again. The potentials were varied from -0.36 to -0.42 V versus reference electrode. For As^{V} concentration 20 μgl^{-1}, 400 mgl^{-1} Cu^{II} and 3.2 mM thiosulfate, the results are shown in Table 3-22 and Figure 3-14. The results indicated that deposition potential of -0.39 V gave the best signal for TAs determinations and was further used for TAs determination.

Table 3-22 Influence of deposition potential on TAs peak height ($E_{1/2}$ ≈ -0.680 to -0.724 V)

Deposition potential (V)	Peak height (μA)	%RSD
-0.36	1.865	1.1
-0.37	3.270	3.3
-0.38	3.960	5.0
-0.39	9.901	3.7
-0.40	8.898	4.3
-0.41	9.031	6.3
-0.42	2.177	9.5

[a] Values given are means (n=3).

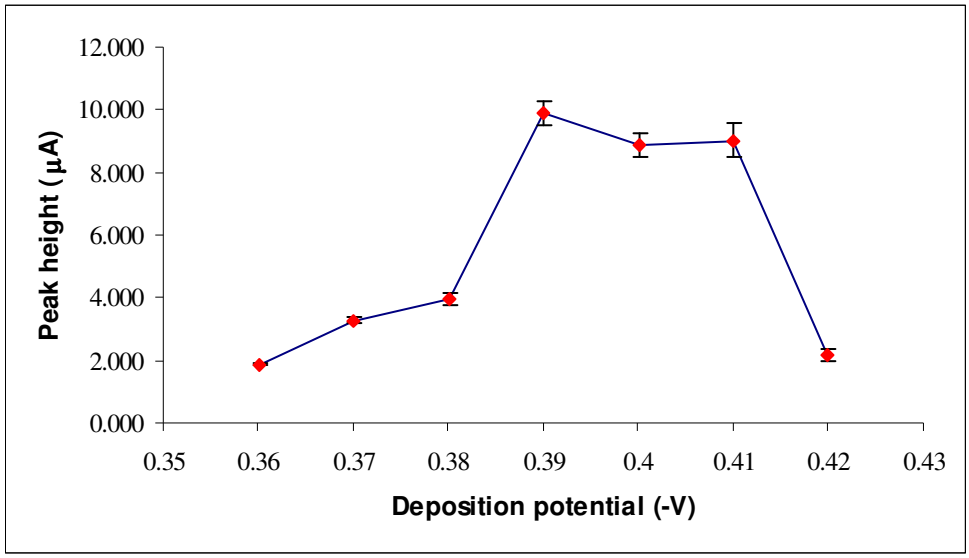

Figure 3-14 Influence of deposition potential on TAs peak height ($E_{1/2}$ ≈ -0.680 to -0.724 V)

3.4.2 Deposition time

To increase peak current and improve method sensitivity, the influence of deposition time was also investigated. In the first step, the deposition times for As^{III} determination

were tested. For As^{III} concentration 20 μgl^{-1} and 50 mgl^{-1} Cu^{II}, deposition time between 0-240 s were evaluated. The influence of deposition time is illustrated in Table 3-23 and Figure 3-15. It was found that deposition time greater than 30 s caused a reduction in As peak height. For deposition times up to 30 s, the peak was sharp and symmetrical and the peak height increased with time. For longer deposition times (>30 s), the peak became broader and lower. All results are consistent with those from the previous study of Ferreira and Barros which stated that the higher the Cu^{II} concentration the lower the accumulation time needed to achieve maximum current (Ferreira and Barros, 2002). This can be due to the formation of a different intermetallic compound. Different stoichiometry between Cu and As (Cu_xAs_y) can be formed depending on the experimental conditions such as nature and concentration of supporting electrolyte, Cu concentration and deposition potential (Profumo *et al*., 2005).

Table 3-23 Influence of deposition time on As^{III} peak height

Deposition time (s)	Peak height (μA)	%RSD
0	0.000	0.0
15	0.355	5.0
30	5.405	4.6
45	2.070	1.3
60	1.443	6.4
75	1.031	3.1
90	1.016	4.8
120	0.976	9.3
150	0.901	9.4
180	0.885	7.8
240	0.382	9.6

[a] Values given are means (n=3).

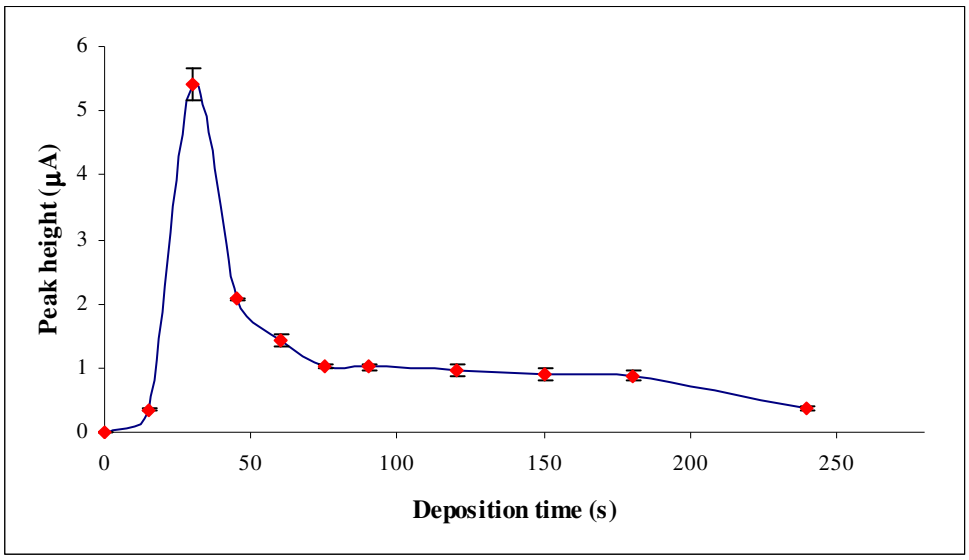

Figure 3-15 Influence of deposition time on As^{III} peak height

In case of TAs determination, SWCSV deposition times were also investigated with 10 ml samples containing 20 μgl^{-1} As^{V}, 400 mgl^{-1} Cu^{II} and 3.2 mM thiosulfate with the deposition time varied from 30-390 s. The results are shown in Table 3-24 and Figure 3-16. The peak current increases continuously with the increase of deposition time and slightly increase at the time higher than 240s, different from that observed in the determination of As^{III}. Therefore, the deposition time of 240 s was chosen. Moreover, this time was selected for routine analysis in order to keep the time of analysis relatively short.

Table 3-24 Influence of deposition time on TAs peak height

Deposition time (s)	Peak height (μA)	%RSD
30	0.581	0.3
60	1.640	3.3
90	2.871	3.0
120	3.620	2.7
150	4.604	0.1
180	5.630	0.9
210	6.051	3.0
240	7.365	4.5
270	7.860	0.6
300	9.049	0.6
330	9.201	0.0
360	9.859	0.5
390	10.231	3.1

[a] Values given are means (n=3).

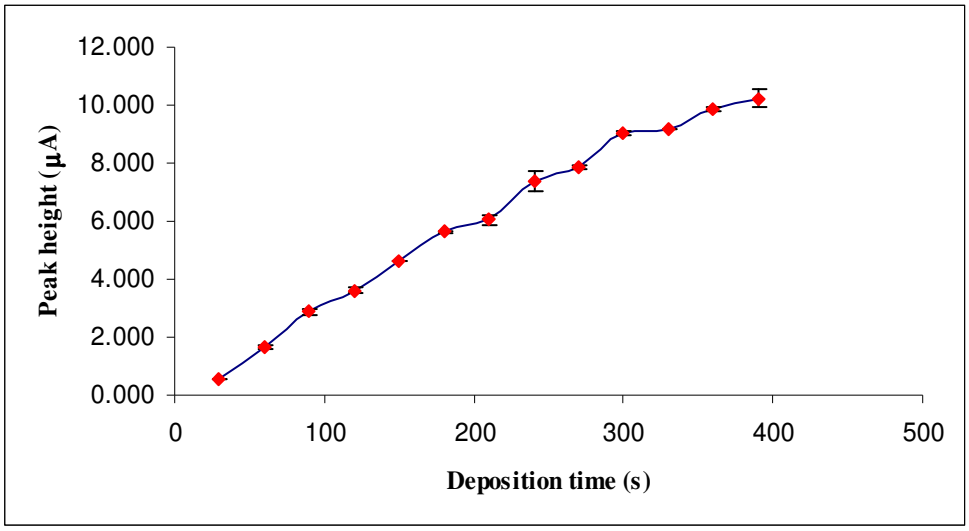

(a)

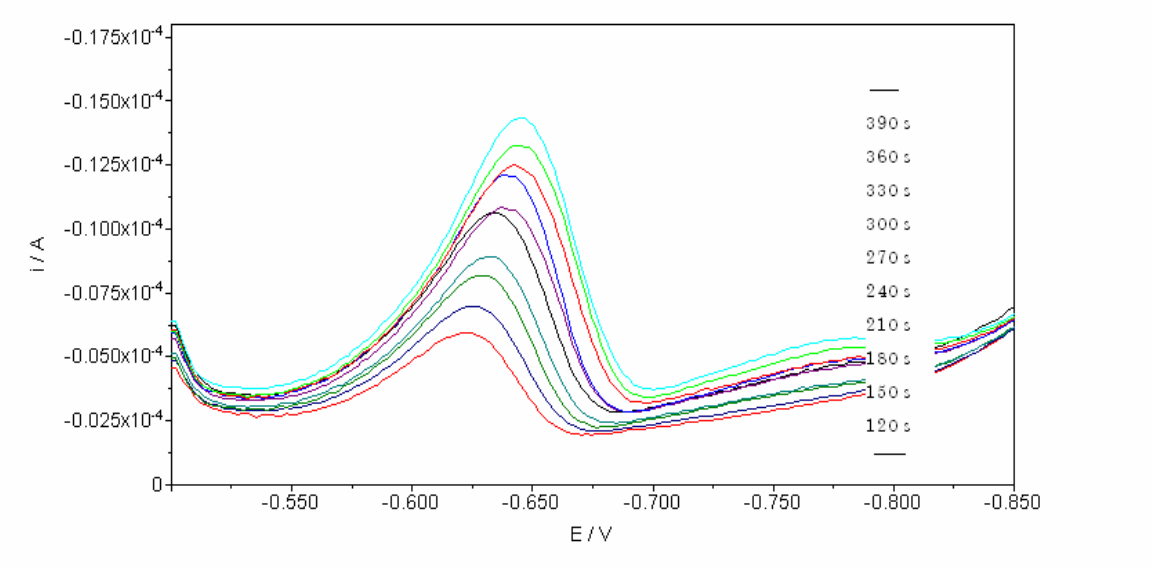

(b)

Figure 3-16 Influence of deposition time on TAs peak height; (a) the graph plotting between peak current versus deposition time and (b) voltammograms of varied deposition time (120-390 s)

3.4.3 HCl concentration

In previous studies of several researchers, it was found that chloride plays an important role in the process of deposition of an intermetallic compound (Cu_xAs_y) on electrode. The function of chloride is to stabilize Cu^{I} formed in an intermediate step while As^{III} is reduced to As according to the following reaction:

Accumulation step: $As + 3CuCl_3^{2-} + 3e^- \rightarrow Cu_3As + 9Cl^-$ (3-1)

Stripping step: $Cu_3As + 3H^+ + Hg + 3e^- \rightarrow Cu(Hg) + AsH_3$ (3-2)

The high concentration of chloride at the electrode surface can increase the amount of As-Cu compound deposited, whereas too much concentration of chloride can cause positive shift of peak current because it favors the reductions of As^{III} and Cu^{II} (Smart *et al*., 1996; Ferreira and Barros, 2002 and Profumo *et al*., 2005). In this work the concentrations of HCl as

supporting electrolyte were examined. HCl concentrations varied from 0.0-5.0 M were tested. The influence of HCl concentrations on As peak height is illustrated in Table 3-25 and Figure 3-17. The best result was obtained with HCl concentration of 2.0 M which was therefore used throughout following experiments.

Table 3-25 Influence of HCl concentration on As peak height

HCl concentration (M)	Peak height (μA)	%RSD
0.0	0.000	0.0
0.5	0.854	4.8
1.0	3.871	3.0
1.5	14.733	4.0
2.0	15.241	6.0
2.5	9.688	1.0
3.0	6.502	7.2
3.5	7.052	3.0
4.0	4.657	5.7
4.5	1.726	8.1
5.0	0.347	8.3

[a] Values given are means (n=3).

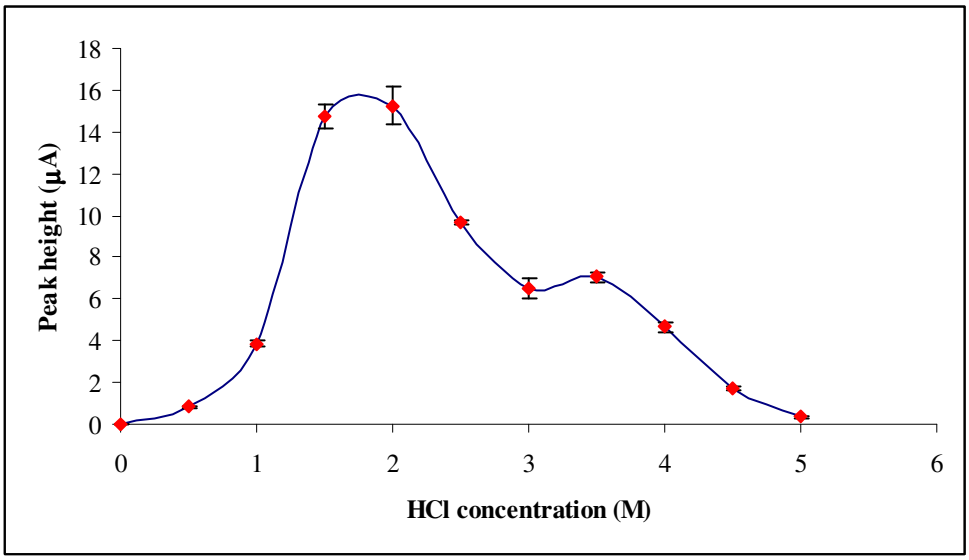

Figure 3-17 Influence of HCl concentration on As peak height

3.4.4 Copper (II) concentration

Since arsenic cannot be electrolytically deposited directly onto a Hg electrode, it is necessary for As^{III} to reacts with Cu^{II} to form an intermetallic compound (Cu_xAs_y) to be able to be deposited onto the HMDE. For selective determination of As^{III}, the amounts of Cu^{II} were investigated by varying concentrations between 0-120 mgl^{-1}. The results were shown in Table 3-26 and Figure 3-18. It was found that, for 20 μgl^{-1} As^{III}, the peak height increased with up to 45 mgl^{-1} Cu^{II} added. Further increase of Cu^{II} greater than 45 mgl^{-1} to 90 mgl^{-1} produced a broad and large single peak and decreased peak height. Higher Cu^{II} led to the disappearance of peak height. The results are consistent with those from the previous study of Ferreira and Barros which stated that the use of Cu^{II} concentrations above 60 mgl^{-1} led to a decrease in the maximum peak current intensity. For this reason, they used less than 50 mgl^{-1} of Cu^{II} concentrations for As^{III} determination (Ferreira and Barros, 2002). This behavior observed was also similar with that found by several other researchers (Profumo *et al*., 2005; He *et al*., 2004). This can due to the formation of an intermetallic compound with a different Cu:As ratio (He *et al*., 2004). Therefore, Cu^{II} concentration of 45 mgl^{-1} was chosen for As^{III} determination.

Table 3-26 Influence of Cu^{II} concentration on As^{III} peak height

Cu concentration (mgl^{-1})	Peak height (μA)	%RSD
0	0.000	0.0
1	0.000	0.0
5	0.030	1.9
15	0.180	1.6
30	4.836	8.9
45	9.727	4.3
60	3.728	2.6
75	2.180	7.6
90	0.343	1.4
105	0.000	0.0
120	0.000	0.0

[a] Values given are means (n=3).

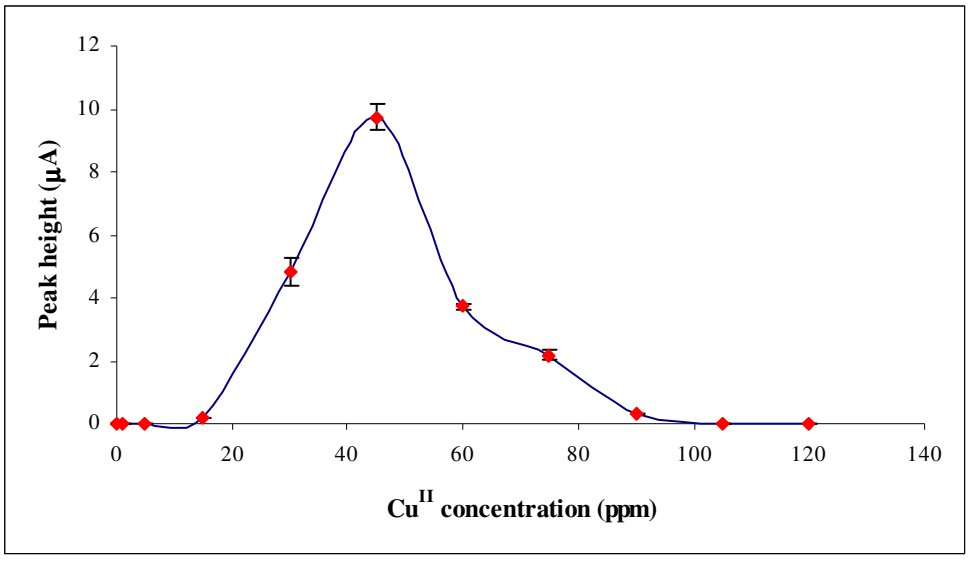

Figure 3-18 Influence of Cu^{II} concentration on As^{III} peak height

For TAs determination, initially the same conditions previously optimized for the determination of As^{III} were adopted (2 M HCl, 45 mgl^{-1} Cu^{II}), with the only difference was that As^{V} was used instead of As^{III}. It was found that in the presence of thiosulfate, Cu^{II} was less efficient in promoting the deposition of As at Hg electrode, a situation that required the use of a much higher concentration of Cu^{II}. Cu^{II} concentrations in the range of 100 to 800 mgl^{-1} were tested. The results were shown in Table 3-27 and Figure 3-19. Maximum peak height was obtained for 600 mgl^{-1} of Cu^{II}. The voltammogram of As (Figure 3-20) reveals that for the concentration of Cu^{II} lower than 600 mgl^{-1}, two peaks were obtained. In contrast, the concentration of Cu^{II} higher than 600 mgl^{-1} led to decreasing single peak height. Therefore, Cu^{II} concentration of 600 mgl^{-1} was chosen for TAs determination.

Table 3-27 Influence of Cu^{II} concentration on TAs peak height

Cu concentration (mgl^{-1})	Peak height (μA)	%RSD
100	5.029	3.4
200	5.216	3.5
300	5.993	6.4
400	6.080	2.9
500	6.869	4.1
600	7.135	1.6
700	6.482	2.0
800	4.864	2.9

[a] Values given are means (n=3).

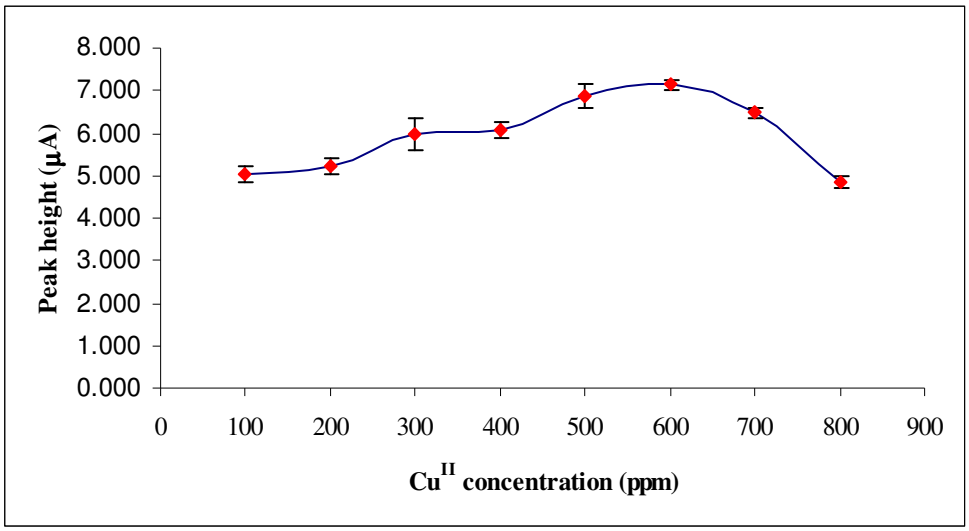

Figure 3-19 Influence of Cu^{II} concentration on TAs peak height.

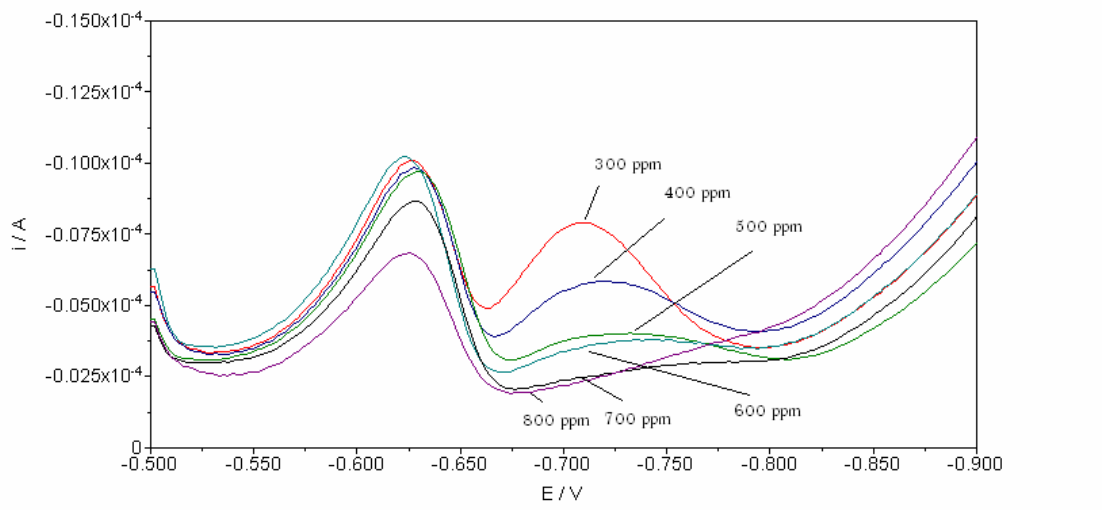

Figure 3-20 Effect of Cu^{II} concentration on the SWCSV determination of 20 μgl^{-1} As^{V}

3.4.5 Reducing agent concentration

After various concentrations of sodium thiosulfate (0, 0.4, 0.8, 1.2, 1.6, 2.0, 2.4, 2.8, 3.0, 3.2, 3.6 and 4.0 mM) were tested to quantitatively reduce As^{V} to As^{III}, the results obtained are shown in Table 3-28 and Figure 3-21. The peak height increased for concentrations of

thiosulfate up to 3.0 mM and then decreased. Therefore, a concentration of 3.0 mM in thiosulfate was chosen (The reduction of As^{V} with thiosulfate prior to the formation of intermetallic compound with Cu^{II} was shown in the reaction 2-4 of chapter 2).

Table 3-28 Influence of thiosulfate concentration on the SWCSV determination of 20 μgl^{-1} of As^{V}

$S_2O_3^{2-}$ concentration (mM)	Peak height (μA)	%RSD
0.0	0.261	8.8
0.4	1.203	5.5
0.8	2.291	4.3
1.2	2.988	6.5
1.6	3.030	6.2
2.0	3.667	6.6
2.4	4.620	1.3
2.8	4.745	0.8
3.0	5.469	1.3
3.2	3.775	5.5
3.6	2.684	1.2
4.0	2.840	3.0

[a] Values given are means (n=3).

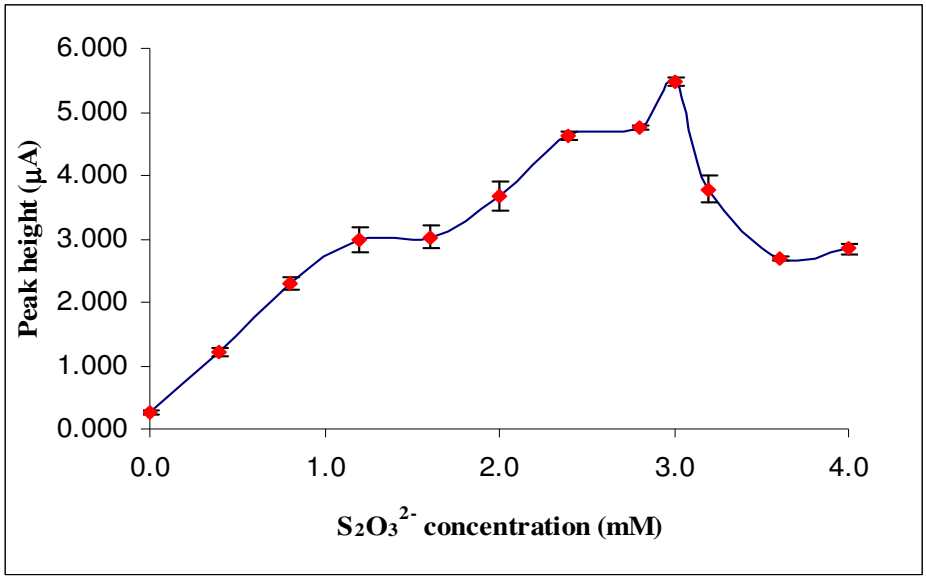

Figure 3-21 The influence of thiosulfate concentration on the SWCSV determination of 20 μgl^{-1} of As^{V}

3.4.6 Reducing time

To determine the time required to quantitatively reduce As^{V} to As^{III}, the reduction time was varied from 5-30 min (5, 10, 20 and 30 min) for a 10 ml sample with 3 mM thiosulfate and 20 μgl^{-1} As^{V}. As shown in Table 3-29 and Figure 3-22, it can be seen that the minimum time required to obtain a reasonable voltammogram with 3 mM thiosulfate was 10 min. Additionally, As response was stable for reduction times greater than 10 min. Thus, the reduction time of 10 min was chosen to allow quantitative reduction of As^{V} to As^{III} in the 10 ml sample solution.

Table 3-29 Effect of reduction time for conversion of As^{V} to As^{III} with addition of 3 mM thiosulfate to a sample containing 20 μgl^{-1} As^{V}

Reducing times (min)	Peak height (μA)	%RSD
5	12.074	1.5
10	14.078	0.8
20	14.246	3.2
30	14.302	2.4

[a] Values given are means (n=3).

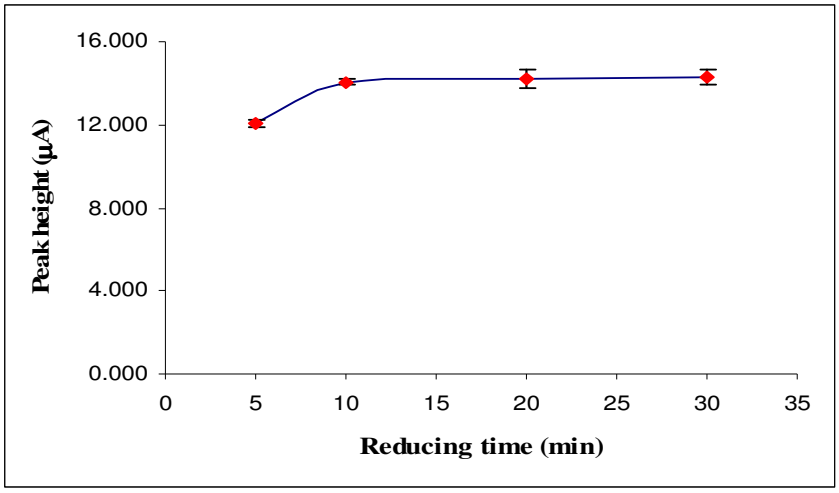

Figure 3-22 Effect of reduction time for conversion of As^{V} to As^{III} with addition of 3 mM thiosulfate to a sample containing 20 μgl^{-1} As^{V}

3.4.7 Efficiency of As^{V} to As^{III} conversion

To evaluate the efficiency of reduction of As^{V} to As^{III}, three compositions of 20 μgl^{-1} As (total) solutions (20/0, 10/10, and 0/20 μgl^{-1} for As^{III}/As^{V} ratios) were tested. As can be seen in Table 3-30 and Figure 3-22, the shapes and heights of the peaks are very similar (a

2.5% RSD of the mean of three measurements was obtained), and it can be concluded that the reduction of As^{V} to As^{III} is quantitative.

Table 3-30 Efficiency of thiosulfate on the reduction of As^{V} to As^{III}

As^{III}:As^{V} ratio (μgl^{-1})	%recovery of As	%RSD
20:0	100	2.3
10:10	102	9.3
0:20	97	7.4

[a] Values were given as mean (n=3, n represents three replicates in each case).

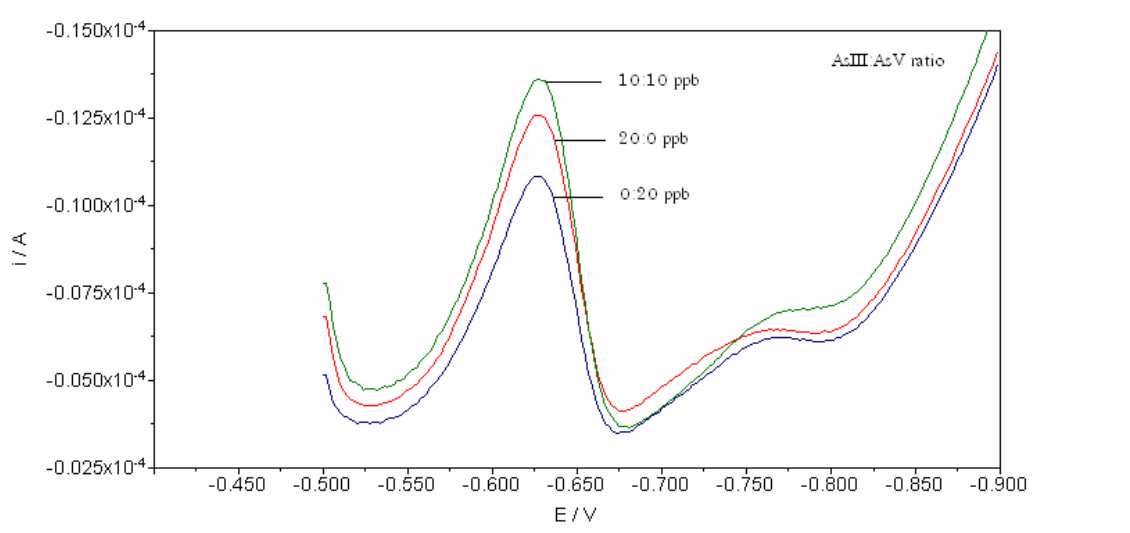

Figure 3-23 Efficiency of thiosulfate on the reduction of As^{V} to As^{III}.

3.5 Analytical performances data for SWCSV

3.5.1 Linear range

The linear range is determined by plotting the peak height versus the concentration of As standard solution. It is desirable to work within the linear region of the resulting calibration curve.

3.5.1.1 Linear range of As^{III} detection

The calibration graph of As^{III} at various concentrations (0-100 μgl^{-1}) is shown in Table 3-31 and Figure 3-23 (a). It was found that the curve was linear from 0 to at least 70 μgl^{-1} with the correlation coefficient (r^2) of 0.9942 as shown in Figure 3-23 (b) and gradually became non linear with increasing of As concentrations.

Table 3-31 The peak height of As^{III} detection at different As^{III} concentrations

As^{III} concentration (μgl^{-1})	Peak height (μA)[a]	%RSD[a]
0	0.000	0.0
10	7.503	1.7
20	15.750	0.9
30	22.043	0.9
40	28.557	3.1
50	37.665	0.2
60	40.822	4.9
70	47.725	2.4
80	50.432	5.2
90	53.119	5.7
100	58.633	5.3

[a] Values given are means (n=3).

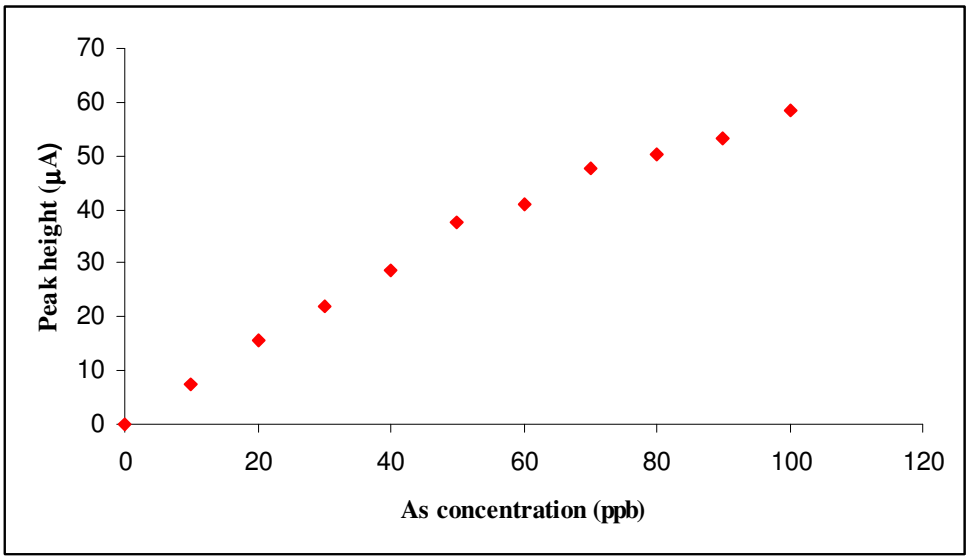

(a)

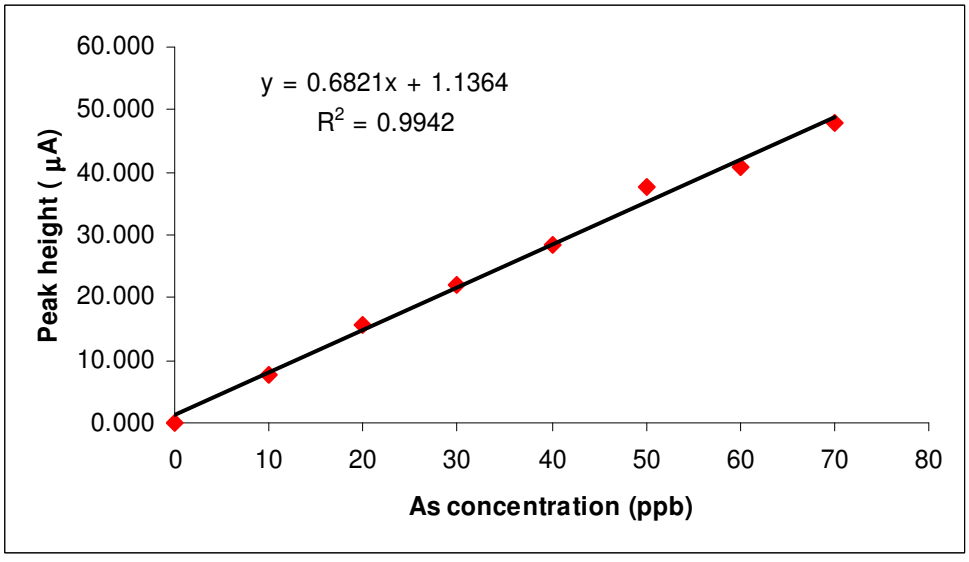

(b)

Figure 3-24 The calibration graph of As^{III} at the different concentrations; (a) 0-100 μgl^{-1} and (b) 0-70 μgl^{-1}

3.5.1.2 Linear range of TAs detection

The calibration graph of TAs at various concentrations (0-100 μgl^{-1}) is shown in Table 3-32 and Figure 3-24 (a). It was found that the curve was linear from 0 to at least 100 μgl^{-1} with the correlation coefficient (r^2) of 0.9981 as shown in Figure 3-24 (b) and gradually became non linear with increasing of As concentrations.

Table 3-32 The peak height of TAs detection at different As^V concentrations

As^V concentration (μgl^{-1})	Peak height (μA)[a]	%RSD[a]
0	0.000	0.0
10	3.906	2.5
20	8.240	2.6
30	12.141	1.4
40	16.673	0.7
50	19.595	1.8
60	23.245	3.1
70	27.022	5.5
80	31.048	1.7
90	34.424	0.4
100	40.176	0.6
110	39.747	1.5
120	42.062	1.4
130	45.446	0.9
140	47.275	0.5
150	50.235	0.6

[a] Values given are means (n=3).

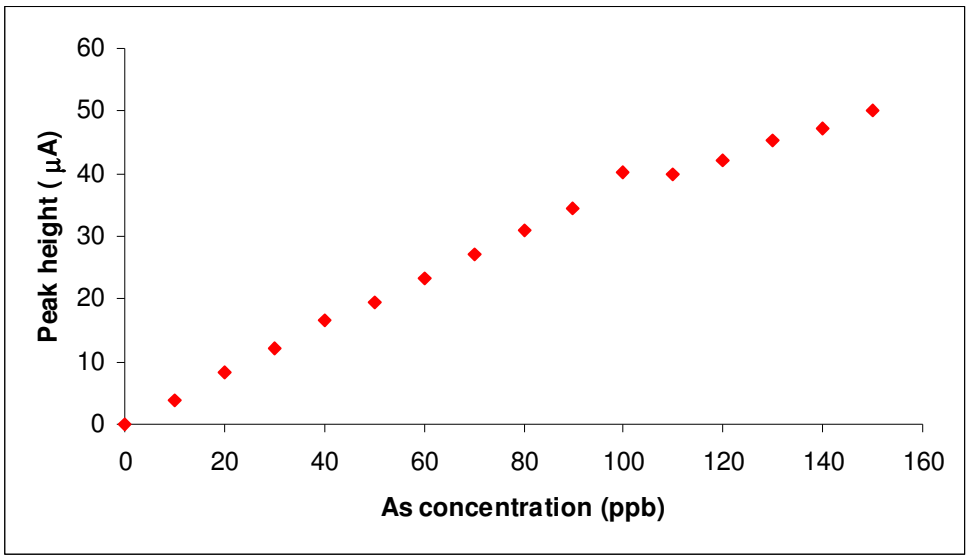

(a)

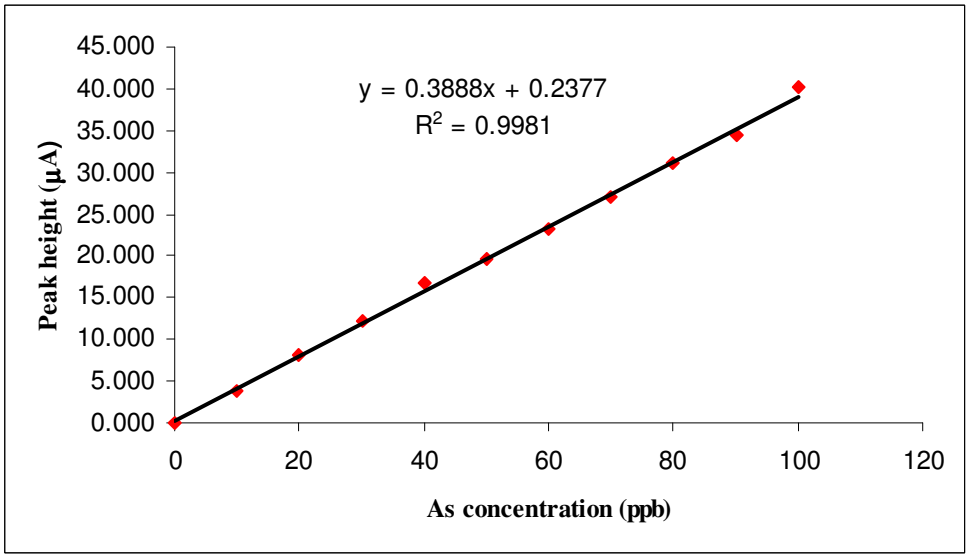

(b)

Figure 3-25 The calibration graph of As^{V} at the different concentrations; (a) 0-150 μgl^{-1} and (b) 0-100 μgl^{-1}

3.5.2 Limit of detection (LOD) and Limit of quantification (LOQ)

The limits of detection (LOD) and limits of quantitative (LOQ) of As^{III} and TAs were studied by measuring the absorbance of ten replications of the blank. The limits of detection and limits of quantitative were calculated following section 2.6.2 and 2.6.3, respectively (Coelho *et al*., 2002).

The results for evaluating LOD and LOQ of As^{III} and TAs are shown in Table 3-33 and Table 3-34, respectively.

3.5.2.1 LOD and LOQ of As^{III} determination

When ten blanks spiked with 0.1 μgl^{-1} of As standard solution were measured and the slope from calibration graph was obtained (as shown in Figure 3-25), it was found that the LOD and LOQ of As^{III} were 0.5 and 1.6 μgl^{-1}, respectively (Table 3-34).

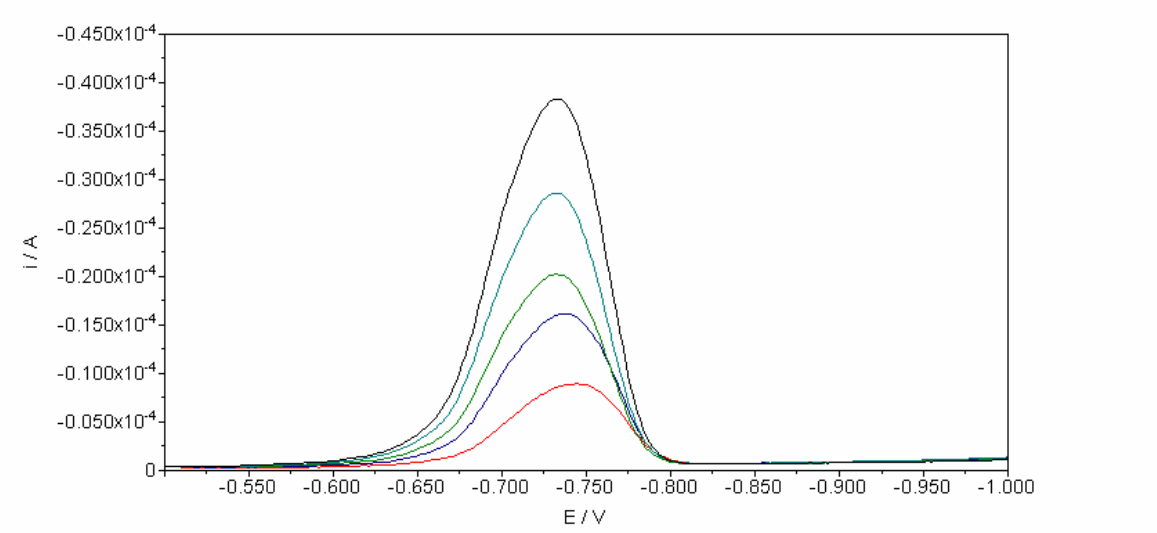

Figure 3-26 Voltammetric curves of 10, 20, 30, 40 and 50 μgl^{-1} As^{III} for plotting the calibration curve

Table 3-33 The determination of 10 blanks for LOD and LOQ quantification (As^{III}); SWCSV

Replicate	**Peak height (μA)**	
1	0.338	
2	0.409	
3	0.325	
4	0.418	
5	0.681	
6	0.553	
7	0.454	
8	0.593	
9	0.488	
10	0.509	
Average	**0.477**	
SD (σ)	**0.112**	
Calibration Slope (m)	**0.714**	
LOD (3σ/m)	**0.5**	**(μgl^{-1})**
LOQ (10σ/m)	**1.6**	**(μgl^{-1})**

3.5.2.2 LOD and LOQ of TAs determination

In case of TAs, when ten blanks spiked with 0.1 μgl^{-1} of As standard solution were measured and the slope from calibration graph was obtained (as shown in Figure 3-26), it was found that the LOD and LOQ of TAs were 0.4 and 1.5 μgl^{-1}, respectively (Table 3-35).

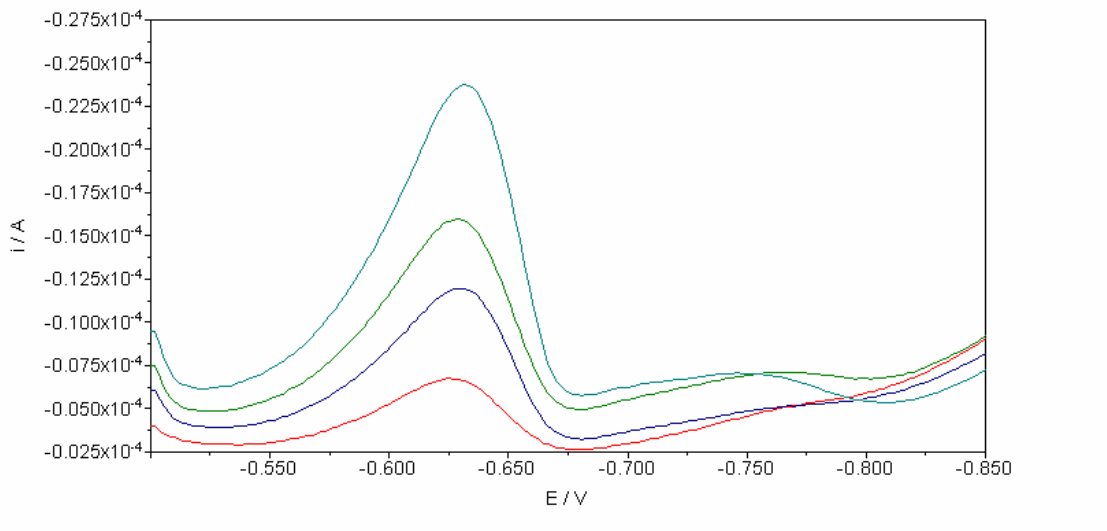

Figure 3-27 Voltammetric curves of 10, 20, 30 and 40 μgl^{-1} TAs for the calibration curve

Table 3-34 The 10 times determination of blanks for LOD and LOQ quantification (TAs); SWCSV

Replicate	**Peak height (μA)**	
1	0.297	
2	0.127	
3	0.124	
4	0.209	
5	0.195	
6	0.177	
7	0.138	
8	0.204	
9	0.258	
10	0.201	
Average	**0.193**	
SD (σ)	**0.056**	
Calibration Slope (m)	**0.388**	
LOD (3σ/m)	**0.4**	**(μgl^{-1})**
LOQ (10σ/m)	**1.5**	**(μgl^{-1})**

3.5.3 Accuracy and precision

The accuracy of this investigation method was evaluated from the determination of certified reference material (CTA-VTL-2). Good quality control data for analysis of arsenic were obtained (Table 3-35).

Table 3-35 The experimental and certified values for As determination in the CRM by using SWCSV

Sample	**Certified value (μgg^{-1})**	**Determined value (μgg^{-1})**	**%recovery**
CTA-VTL-2	0.969 ± 0.072	0.949 ± 0.021	98

From the results in Table 3-35, total acid-digested arsenic determination, the measured value for As in CTA-VTL-2 (Virginia Tobacco Leaves) was 0.949 ± 0.021 μgg^{-1}, which was in agreement with the certified value (0.969 ± 0.072 μgg^{-1}). The recovery of As was 98%.

However, for inorganic arsenic speciation, no certified value of concentration has been provided for arsenic species. Therefore, the recovery values of inorganic species were quantified by spiking 20 and 30 μgl^{-1} of As^{III} and As^{V} to samples. As shown in Table 3-36, the recovery values for As^{III} and As^{V} were in agreement with the value of spiked samples.

Table 3-36 Experimental recovery on arsenic determination by SWCSV in edible plant samples spiked with 20 and 30 μgl^{-1} of As^{III} and As^{V}

	As^{III}		As^{V}	
	Conc.(μgl^{-1})	Recovery (%)	Conc. (μgl^{-1})	Recovery (%)
Sample	ND	-	ND	-
Sample+20 μgl^{-1}	19.6	98.0	18.7	93.5
Sample+30 μgl^{-1}	28.1	93.7	28.4	94.7

In addition, the precision of the analysis method was also evaluated as %RSD of ten replication measurements. The %RSD of 10 μgl^{-1} As^{III} and TAs determinations obtained from this method were 4.0 and 4.9%, respectively. The results are shown in Table 3-37 and 3-38.

Table 3-37 The determination of 10 μgl^{-1} As^{III} for evaluating the precision (SWCSV)

Replicate	**Peak height (μA)**
1	3.069
2	3.086
3	3.029
4	2.986
5	2.995
6	2.729
7	2.843
8	2.906
9	3.000
10	2.826
Average	**2.947**
SD	**0.117**
%RSD	**4**

Table 3-38 The determination of 10 μgl^{-1} TAs for evaluating the precision (SWCSV)

Replicate	**Peak height (μA)**
1	3.565
2	3.799
3	3.221
4	3.669
5	3.817
6	3.793
7	3.750
8	3.743
9	3.775
10	3.749
Average	**3.688**
SD	**0.180**
%RSD	**5**

3.6 Determination of As species in edible plant samples using SWCSV

For the determination of arsenic concentration in samples, first of all concentrations of the arsenic species in all the extracted and digested samples were calculated using both external calibration and standard addition methods. As shown in Appendix D-5, it was found that significant differences were observed between the slopes of the external calibration and the standard addition calibration lines (*t*-test, $P<0.05$). Therefore, the standard addition method was used to determine the arsenic in samples to minimize the effect of the chemical composition of the matrix.

The studied method was applied to determination of As species in two types of edible plants (Lemon grass and Turmeric) collected from arsenic contaminated area, Ron Phibun

sub-district, Ron Phibun district, Nakhon Si Thammarat province. The content of different arsenic species in the above mentioned edible plant samples were summarized in Table 3-39 and 3-40.

Table 3-39 Concentrations of total-As and inorganic arsenic species in Lemon grass (as $\mu g g^{-1}$ dry weight, mean±SD); SWCSV

Villages/point	As^{III}	As^{V}	Total water-extracted As[a]	Total acid-digested As[b]
M.1/1	ND[c]	ND	ND	0.351±0.025
M.1/2	ND	ND	ND	0.289±0.030
M.1/3	ND	ND	ND	0.294±0.035
M.1/4	ND	ND	ND	0.333±0.038
M.1/5	ND	ND	ND	0.339±0.002
M.2/1	ND	ND	ND	0.348±0.021
M.2/2	ND	ND	ND	0.152±0.002
M.2/3	ND	ND	ND	0.331±0.002
M.2/4	0.356±0.039	0.074±0.039	0.430±0.071	1.078±0.032
M.2/5	ND	ND	ND	0.437±0.034
M.13/1	ND	ND	ND	0.368±0.011
M.13/2	ND	ND	ND	0.258±0.004
M.13/3	ND	ND	ND	0.108±0.002
M.13/4	ND	ND	ND	0.194±0.002
M.13/5	ND	ND	ND	0.190±0.002

[a] Total water-soluble inorganic arsenic species (As^{III} + As^{V}) extracted by water.

[b] Total arsenic was determined by digesting samples with a $HNO_3/HClO_4/H_2SO_4$ mixture at 100 ^{o}C.

[c] ND = not detected.

Table 3-40 Concentrations of total-As and inorganic arsenic species in Turmeric (as $\mu g g^{-1}$ dry weight, mean±SD); SWCSV

Villages/point	As^{III}	As^{V}	Total water-extracted As[a]	Total acid-digested As[b]
M.1/1	ND[c]	ND	ND	0.528±0.001
M.1/2	ND	ND	ND	0.341±0.018
M.1/3	ND	ND	ND	0.334±0.001
M.1/4	ND	ND	ND	0.633±0.023
M.1/5	ND	ND	ND	0.648±0.013
M.2/1	ND	ND	ND	0.483±0.032
M.2/2	ND	ND	ND	0.908±0.058
M.2/3	ND	ND	ND	0.566±0.006
M.2/4	ND	ND	ND	0.556±0.012
M.2/5	ND	ND	ND	1.607±0.039
M.13/1	ND	ND	ND	0.454±0.022
M.13/2	ND	ND	ND	1.181±0.116
M.13/3	ND	ND	ND	0.570±0.013
M.13/4	ND	ND	ND	0.375±0.010
M.13/5	0.395±0.019	0.269±0.195	0.664±0.185	1.931±0.189

[a] Total water-soluble inorganic arsenic species (As^{III} + As^{V}) extracted by water.

[b] Total arsenic was determined by digesting samples with a $HNO_3/HClO_4/H_2SO_4$ mixture at 100 ^{o}C.

[c] ND = not detected.

Table 3-39 and Table 3-40 revealed that the concentration of inorganic arsenic species (As^{III}, As^{V} and total water-extracted As) in most samples were too low, less than LOD values, leading to be none detectable. To solve this problem, the amounts of extracted samples were increased up to 10 times (≈1.000 g) and it was found that SWCSV was able to detect

inorganic arsenic species (As^{III} and As^{V}) in only one sample of each type of edible plant samples. In the case of total acid-digested arsenic determination, the amounts of digested samples needed to be increased (≈2.500 g) to be detectable, it was found that no significant differences were observed (*t*-test, $P<0.05$), in some samples (more than 50% of all samples), between the total acid-digested arsenic concentration obtained by FI-HG-AAS and SWCSV (Appendix D-6). However, at the 99.9% confidence level (t-test, $P<0.001$) no significant differences were observed in all samples.

3.7 A comparison between FI-HG-AAS and SWCSV for inorganic arsenic speciation

As shown in Table 3-41, there is a significant difference in the ability of the two methods to measure inorganic arsenic species. The SWCSV method showed poor sensitivity for trace amount of inorganic arsenic species detections in samples while HG-AAS showed excellent sensitivity for both arsenic species. SWCSV was able to detect inorganic species (As^{III} and As^{V}) in only one sample of each type of edible plant samples because of its high limit of detection (>0.4 μgl^{-1} for both As species). For total acid-digested arsenic determination by SWCSV, the amounts of digested samples needed to be increased to reach LOD value and it was found that there was similarity between total acid-digested arsenic values obtained by using FI-HG-AAS and SWCSV technique (*t*-test in Appendix D-6) in edible plant samples and certified reference material (CTA-VTL-2)

Moreover, the comparative study of two methods also found that each method has its own merits (Table 3-42) and limitations. The method of choice will depend on instrument availability, sensitivity and running cost. HG-AAS is well known to be popular method of As speciation because of its sensitivity and selectivity but suffers with high costs and laborious sample preparation. Moreover, HG-AAS has limited linearity to the concentration of only 50 μgl^{-1} and it is recommended for analyte with low concentrations (Akter *et al*., 2005). CSV, especially in the SWCSV mode, is a simple, new, cheap, selective and less labor technique but limited by its poor sensitivity (high LOD and LOQ). Although, CSV suffers with LOD value, it can provide wide linear range which can go up 100 μgl^{-1}that consists strongly with investigation by Greulach and Henze in 1995 (Greulach and Henze, 1995).

Table 3-41 A comparison between FI-HG-AAS and SWCSV techniques for arsenic speciation in edible plants samples (as $\mu g g^{-1}$ dry weight)

Sample ID/ Mode		Lemongrass				Turmeric			
		As^{III}	As^{V}	Total water-extracted As	Total acid-digested As	As^{III}	As^{V}	Total water-extracted As	Total acid-digested As
M1/1	I[a]	0.026	0.114	0.140	0.238	0.041	0.064	0.105	0.601
	II[b]	ND[c]	ND	ND	0.351	ND	ND	ND	0.528
M1/2	I	0.020	0.102	0.122	0.226	0.026	0.065	0.091	0.365
	II	ND	ND	ND	0.289	ND	ND	ND	0.341
M1/3	I	0.031	0.092	0.123	0.316	0.025	0.086	0.091	0.290
	II	ND	ND	ND	0.294	ND	ND	ND	0.334
M1/4	I	0.038	0.213	0.251	0.304	0.023	0.105	0.128	0.623
	II	ND	ND	ND	0.333	ND	ND	ND	0.633
M1/5	I	0.036	0.093	0.129	0.247	0.053	0.157	0.210	0.660
	II	ND	ND	ND	0.339	ND	ND	ND	0.648
M2/1	I	0.034	0.091	0.125	0.381	0.020	0.144	0.110	0.468
	II	ND	ND	ND	0.348	ND	ND	ND	0.482
M2/2	I	0.038	0.058	0.096	0.231	0.162	0.144	0.306	0.997
	II	ND	ND	ND	0.152	ND	ND	ND	0.908
M2/3	I	0.049	0.065	0.114	0.301	0.026	0.059	0.085	0.563
	II	ND	ND	ND	0.331	ND	ND	ND	0.566
M2/4	I	0.385	0.061	0.446	0.979	0.075	0.076	0.151	0.557
	II	0.356	0.074	0.430	1.078	ND	ND	ND	0.556
M2/5	I	0.040	0.068	0.108	0.465	0.021	0.130	0.151	1.384
	II	ND	ND	ND	0.437	ND	ND	ND	1.608
M13/1	I	0.022	0.094	0.116	0.339	0.024	0.066	0.090	0.497
	II	ND	ND	ND	0.368	ND	ND	ND	0.454
M13/2	I	0.023	0.120	0.143	0.281	0.026	0.090	0.116	1.077
	II	ND	ND	ND	0.258	ND	ND	ND	1.181
M13/3	I	0.010	0.106	0.116	0.148	0.088	0.199	0.287	0.597
	II	ND	ND	ND	0.108	ND	ND	ND	0.570
M13/4	I	0.036	0.066	0.102	0.175	0.038	0.088	0.126	0.396
	II	ND	ND	ND	0.194	ND	ND	ND	0.375
M13/5	I	0.022	0.114	0.136	0.197	0.331	0.146	0.480	1.873
	II	ND	ND	ND	0.190	0.395	0.269	0.664	1.931

[a] I = FI-HG-AAS technique; [b] II = SWCSV technique; [c] ND = not detected.

Table 3-42 Performance of FI-HG-AAS and SWCSV method

	FI-HG-AAS	
	As^{III}	**TAs**
Linear regression equation	y=0.2694x-0.0012	y=0.2462x+0.1254
Linear range (μgl^{-1})	0-20	0-20
Correlation coefficient (r^2)	0.9985	0.9955
Limit of detection (μgl^{-1})	0.02	0.03
Limit of quantification (μgl^{-1})	0.07	0.10
Precision (%RSD)	2	4
	SWCSV	
Linear regression equation	y=0.6821x+1.1364	y=0.3818x+0.4488
Linear range (μgl^{-1})	0-70	0-100
Correlation coefficient (r^2)	0.9942	0.9987
Limit of detection (μgl^{-1})	0.5	0.4
Limit of quantification (μgl^{-1})	1.6	1.5
Precision (%RSD)	4	5

From this study, it may be stated that CSV is considered to be promising and alternative method for inorganic arsenic speciation in biological samples. However, these samples have to be contain arsenic much highly enough to be in above mentioned LOD values.